Global sensitivity analysis of reactor parameters

Bolade Adewale Adetula

21540330

Mini-dissertation submitted in partial fulfilment of the requirements for the degree of Master of Science in Nuclear Engineering at the Potchefstroom campus of the North-West University

Supervisor: Prof E. Mulder

North-West University, Department of Nuclear Engineering

Potchefstroom, Private Bag X6001, South Africa.

Co-supervisor: Dr P. Bokov

South African Nuclear Energy Corporation

Pelindaba, Pretoria, South Africa.

May 4, 2011

Contents

List of Figures

List of Tables

Abstract

Calculations of reactor parameters of interest (such as neutron multiplication factors, decay heat, reaction rates, etc.), are often based on models which are dependent on groupwise neutron cross sections. The uncertainties associated with these neutron cross sections are propagated to the final result of the calculated reactor parameters. There is a need to characterize this uncertainty and to be able to apportion the uncertainty in a calculated reactor parameter to the different sources of uncertainty in the groupwise neutron cross sections, this procedure is known as sensitivity analysis. The focus of this study is the application of a modified global sensitivity analysis technique to calculations of reactor parameters that are dependent on groupwise neutron cross-sections. Sensitivity analysis can help in identifying the important neutron cross sections for a particular model, and also helps in establishing best-estimate optimized nuclear reactor physics models with reduced uncertainties.

In this study, our approach to sensitivity analysis will be similar to the variance-based global sensitivity analysis technique, which is robust, has a wide range of applicability and provides accurate sensitivity information for most models. However, this technique requires input variables to be mutually independent. A modification to this technique, that allows one to deal with input variables that are block-wise correlated and normally distributed, is presented.

The implementation of the modified technique involves the calculation of multi-dimensional integrals, which can be prohibitively expensive to compute. Numerical techniques specifically suited to the evaluation of multidimensional integrals namely Monte Carlo, quasi-Monte Carlo and sparse grids methods are used, and their efficiency is compared. The modified technique is illustrated and tested on a two-group cross-section dependent problem. In all the cases considered, the results obtained with sparse grids achieved much better accuracy, while using a significantly smaller number of samples.

Keywords: Monte Carlo, quasi-Monte Carlo, sparse grids, global sensitivity analysis, groupwise, neutron cross-sections.

Dedication

This mini-dissertation is dedicated to my beloved daughter Adebola Chuma Adetula.

Acknowledgements

I wish to express my profound gratitude to my supervisors Prof Eben Mulder and in particular Dr Pavel Bokov for his assistance and patient guidance throughout my study. Funding and permission to study from the management of Necsa is greatly appreciated.

I am also greatly indebted to members of the Radiation and Reactor Theory group of Necsa, for the help and useful discussions I received during the write up of this mini-dissertation. In particular I would like to express my gratitude to Johann van Rooyen and Hantie Labuschagne for proofreading this mini-dissertation. Lastly, I wish to thank Nothemba, Chuma, my parents and all my family members for their support.

Chapter 1

Introduction

Models are developed to approximate systems and processes in the real world. There is the need for a model to be reliable, and there should be confidence in the model and the results produced by it. However, assumptions and *uncertainties* associated with the input data of a model are propagated to the output of the model. The uncertainties in the input are often expressed in terms of the covariance or correlation matrix. The propagation of uncertainties from the input to the output of a model is known as *uncertainty analysis*. The apportioning of uncertainty in the output of a model (numerical or otherwise) to different sources of uncertainty in the model input, is known as *sensitivity analysis* [1], and the associated quantitative values are known as *sensitivity indices*. The sensitivity indices can be used to rank the input variables of the model, based on the influence they have on the output. It thus becomes possible to recognize the statistically insignificant/unessential input variables that exert little influence on the output. This allows for the reduction of the dimensionality of the problem by fixing the unessential input variables. More experiments, computations and research can also be done to determine the essential input variables with a higher degree of accuracy. Hence, sensitivity analysis serves as a guide for model construction by assessing methods used for reducing uncertainties.

Sensitivity analysis methods can be classified in two broad categories [2]:

1. **Local Sensitivity Analysis (LSA)**. They are usually based on derivatives, and analyse the behaviour of the model output around a chosen point. LSA methods are capable of dealing with linear models, because the property at a point away from the chosen point can

be computed quickly by linear extrapolation using first order derivatives. They are efficient in computer time, however, they do not provide for an exploration of the full phase space of input parameters, and are not adequate for non-linear models.

2. **Global Sensitivity Analysis (GSA)**. They are techniques used to quantify the influence of uncertain input parameters on the output of a model, by exploring the full phase space of the input parameters. These techniques are usually entropy or variance-based, they can be used to perform accurate quantitative sensitivity analysis and are not restricted to linear models. However, the applications of GSA has been limited. Some major obstacles to the implementation of GSA are (a) the correlation between different input parameters and (b) the curse of dimensionality, which is the exponential growth of computation cost with the number of input parameters. This arises because most of the GSA techniques involve the evaluation of multidimensional integrals whose dimensionality are dependent on the number of input parameters.

Most of the applications of sensitivity analysis to reactor physics have used LSA, which is based on the adjoint flux approach in conjunction with the general perturbation theory applied to the neutron transport equation, a few references among others are [3, 4, 5]. Whilst GSA would be preferred in the application to reactor physics, as it explores the full space of input parameters, its applicability to reactor physics has been very limited [6, 7, 8].

1.1 Background

An extensive literature study has been done, and is given in Chapter 2. The literature study familiarizes the reader with the different sensitivity analysis methods, and their relation to reactor physics. The advantages and disadvantages of sensitivity analysis methods relating to reactor physics were emphasized, and the need for a new methodology to be used for sensitivity analysis relating to reactor physics was shown.

The implementation of GSA can be achieved by using either entropy or variance-based methods. In this study our approach will be based on the Sobol's variance based method [9]. The Sobol's method has received much attention in the scientific community in recent years. The method is robust, has a wide range of applicability and provides accurate sensitivity information for most models as stated in [10, 11]. However, the Sobol's method is defined for statistically independent input variables that are uniformly distributed. The groupwise neutron cross sections that we will consider as input variables are block-wise correlated and normally distributed. In this study, the term groupwise neutron cross sections refers to multigroup or few-group energy dependent neutron cross sections.

1.2 Motivation

Neutron cross sections can be measured experimentally or predicted by nuclear models. The experimentally measured neutron cross sections are combined with predictions of nuclear model calculations, they are then evaluated and processed to arrive at an evaluated set of neutron cross section nuclear data such as found in JENDL, JEFF, ENDF/B, etc. These evaluated data files are often large data grouped by materials and data types, and hence various rules and procedures known as "formats" are required for the computerized storage of such large nuclear data. This often involves the storing of the neutron cross sections, by using data points that can easily be reproduced by polynomial interpolations and functions when needed. The ENDF-6 format [12] is the most widely used format. According to the ENDF-6 formalism, the reaction cross sections versus energy data is stored in file MF 3. Most codes utilized in neutron transport calculations use neutron cross sections that are piece-wise constant over certain energy intervals, called groupwise neutron cross sections. These groupwise neutron cross sections are often described by only their first two statistical moments and are assumed to be normally distributed [13].

In the evaluation of the neutron cross sections and whilst moving (collapsing) from the continuous to the groupwise cross sections, uncertainties in the evaluated neutron cross sections are propagated to the collapsed groupwise cross sections. There exist correlations between the uncertainties of different energy groups of the groupwise neutron cross sections. These uncertainties are expressed in terms of the covariance matrix and are stored in file MF 33 of the ENDF format.

Calculations of reactor parameters of interest (such as neutron multiplication factors, decay heat, reaction rates, etc.), are dependent on groupwise neutron cross sections. The uncertainties associated with the groupwise neutron cross sections are propagated to the final result of the calculated reactor parameters. There is a need to characterize this uncertainty and to be able to apportion the uncertainty in a calculated reactor parameter to the different sources of uncertainty in the groupwise neutron cross sections.

1.3 Purpose of Research

The objective of this study is to develop, implement and test a methodology for the application of GSA to reactor parameters that are dependent on groupwise neutron cross sections. This will help in establishing best-estimate optimized nuclear reactor physics models with reduced uncertainties.

1.4 Outline of the Dissertation

A review of sensitivity analysis techniques and their application to reactor physics, as well as fundamental aspects which are needed for a thorough understanding of the concepts of the proposed GSA technique are contained in Chapter 2. The mathematical formulation of the proposed GSA technique is presented in Chapter 3. Practical methods for implementing the GSA technique and the results obtained from test problems are discussed in Chapter 4.

Chapter 2

Theoretical Background

The uncertainties associated with the input of a model are often propagated to the output of the model. The uncertainties in the output of a model can also be introduced by numerical errors, which are introduced as a consequence of the numerical methods used to solve the equations underlying the mathematical model. The quantification of uncertainty in the output of a model due to the input parameter uncertainties is known as uncertainty analysis, whilst the apportioning of the uncertainty in the output to the different sources of uncertainty in the input is known as sensitivity analysis.

Most of the early considerations of sensitivity analysis were local methods and were merely of mathematical interest. The first systematic mathematical methodology for performing sensitivity analysis were used for linear electrical circuits and was formulated by Bode [14]. Since then, sensitivity analysis has been implemented by several approaches, with the aid of mathematical methods as shown in [15, 16, 17]. The early applications of sensitivity analysis were in the field of optimization and control theory, however, today sensitivity analysis is applied in a broad number of fields such as nuclear [13], socioeconomic [1], biological [18] and others. There are several books on sensitivity analysis that the interested reader is referred to, such as [2, 19, 20, 21, 22]. However, it should be noted as explained in [23] that a precise unified terminology across the various methods for sensitivity indices does not exist. This is because the quantities that are used as a measure of sensitivity indices across the various methods are often different.

In the next section, we will give a brief review of statistical concepts that are relevant to this study. The emphasis of this study is on GSA, however, since most of the applications of sensitivity analysis to reactor physics have been based on LSA methods, we will present a brief overview of LSA methods later in this chapter. Subsequently, we will present a detailed explanation of the various GSA techniques available in literature and highlight their shortcomings, illustrating the need for the new methodology we propose to develop in Chapter 3. An up-to-date review of the relevance and applications of sensitivity analysis (both local and global) to reactor physics will also be presented. Finally, a brief review of some of the methods used for evaluating multidimensional integrals which will be needed in Chapter 4, when implementing the proposed GSA methodology, will be given in the last section of this Chapter.

2.1 Statistical Review

2.1.1 Random Variable

Random variables, as the name implies, are variables that possess a random nature, these variables have an associated probability and they can be either discrete or continuous [24]. Note that in this study, we will use, as it is a rule in statistics, a capital letter to denote a random variable, and a lowercase letter to denote its value (realization). A discrete random variable, maps events to values of a countable set. Consider as an example a discrete random variable X that can possess values $x_1,\ x_2,\ldots,\ x_k$ with a probability of $\mathrm{Prob}(X = x_1),\ \mathrm{Prob}(X = x_2),\ldots,\ \mathrm{Prob}(X = x_k)$. Each probability has a value between zero and one, and the sum of all the probabilities is equal to one. This can be expressed mathematically as, for $i = 1,\ 2,\ldots,\ k$

$$0 \leq \mathrm{Prob}(X = x_i) \leq 1, \quad \text{and} \quad \textstyle\sum_{i=1}^{k} \mathrm{Prob}(X = x_i) = 1. \tag{2.1}$$

On the other hand, a continuous random variable, maps events to values of an uncountable set. Consider as an example, a continuous random variable X, the probability that X lies within a short interval between x and $x + \mathrm{d}x$ is given by $p(x)\mathrm{d}x$. Where $p(x)$ is known as the probability distribution function (pdf) and is a positive function (i.e. $p(x) \geq 0$) which fulfils the normalization condition

$$\int_{-\infty}^{\infty} p(x)\mathrm{d}x = 1. \tag{2.2}$$

A related quantity that completely describes the probability distribution of a random variable is the cumulative distribution function (cdf) denoted by $P(x)$ [25]. This is defined as the probability that a random variable X is less than or equal to some given real number x. If X is a discrete random variable, then the cdf would be given by

$$P(x) = \text{Prob}(X \leq x) = \sum_{x_i \leq x} \text{Prob}(X = x_i). \tag{2.3}$$

However, if X is a continuous random, then the cdf will be given by

$$P(x) = \text{Prob}(X \leq x) = \int_{-\infty}^{x} p(x)\mathrm{d}x. \tag{2.4}$$

2.1.2 Expectation and Variance

The expected value of a random variable is obtained by averaging all possible values that can be attained over its probability measure. The variance of a random variable gives a measure of the amount of variation, from all the possible values that it can attain, with its expected value. Considering a random variable X, if X is discrete and attain values $x_1, x_2, \ldots, x_k$ with probability $\text{Prob}(X = x_i)$ for $i = 1, 2, \ldots, k$, then the expected value μ and variance $\mathsf{V}[X]$ of X are given respectively by

$$\mu = \mathsf{E}[X] = \sum_{i=1}^{k} x_i \text{Prob}(X = x_i), \quad \text{and} \quad \mathsf{V}[X] = \mathsf{E}\left[(X - \mu)^2\right] = \sum_{i=1}^{k} (x_i - \mu)^2 \, \text{Prob}(X = x_i). \tag{2.5}$$

If X is continuous, with probability distribution function $p(x)$, then the expected value μ and variance $\mathsf{V}[X]$ of X are given respectively by

$$\mu = \mathsf{E}[X] = \int_{-\infty}^{\infty} xp(x)\mathrm{d}x, \quad \text{and} \quad \mathsf{V}[X] = \mathsf{E}\left[(X - \mu)^2\right] = \int_{-\infty}^{\infty} (x - \mu)^2 \, p(x)\mathrm{d}x. \tag{2.6}$$

The concept of expectation and variance are also applicable for functions. Consider an arbitrary function of X, $g(X)$ with probability distribution function $p(x)$, then the expected value and variance of $g(X)$ are given respectively by

$$\mathsf{E}[g(X)] = \int_{-\infty}^{\infty} g(x)p(x)\mathrm{d}x, \quad \text{and} \quad \mathsf{V}[g(X)] = \int_{-\infty}^{\infty} (g(x) - \mathsf{E}[g(X)])^2 \, p(x)\mathrm{d}x. \tag{2.7}$$

2.1.3 Mean Vectors, Covariance and Correlation Matrices

A random vector is defined as a vector whose elements are random variables. Suppose $\mathbf{X} = [X_1\ X_2\ \cdots\ X_d]^T$ is a random d-dimensional column vector, where the symbol "T" denotes the transpose operator. The mean vector is given by $\boldsymbol{\mu} = \mathsf{E}[\mathbf{X}] = [\mu_1, \mu_2, \ldots, \mu_d]^T$, the *marginal mean* and variance for each element are defined as $\mu_i = \mathsf{E}[X_i]$ and $\mathsf{V}_{ii} = \mathsf{E}\left[(X_i - \mu_i)^2\right]$, for $i = 1, 2, \ldots, d$. A measure of linear association which provides a measure of how any two random variables X_i, and X_j, vary together is provided by the covariance which is denoted by $\mathsf{Cov}[X_i, X_j]$. Where $\mathsf{Cov}[X_i, X_j] = \mathsf{V}_{ij} = \mathsf{E}[(X_i - \mu_i)(X_j - \mu_j)]$ for $i, j = 1, 2, \ldots, d$.

For a $d-$dimensional column vector $\mathbf{X}$, the variance-covariance matrix consists of d^2 entries, there are d variances V_{ii} for all i, $d(d-1)$ covariances of which $d(d-1)/2$ are independent because of symmetry (i.e $\mathsf{V}_{ij} = \mathsf{V}_{ji}$). The variance-covariance matrix is denoted by $\boldsymbol{\Sigma}$ and is given by

$$\boldsymbol{\Sigma} = \mathsf{E}\left[(\mathbf{X} - \boldsymbol{\mu})(\mathbf{X} - \boldsymbol{\mu})^T\right]. \tag{2.8}$$

The elements of a random vector $\mathbf{X}$ are said to be mutually statistically independent if their joint probability density can be factored as

$$p(\mathbf{x}) = p_{12\cdots d}(x_1, x_2, \ldots, x_d) = p_1(x_1)p_2(x_2)\cdots p_d(x_d), \tag{2.9}$$

for all d-tuples $(x_1, x_2, ..., x_d)$. If any two elements of the random vector $\mathbf{X}$ are statistically independent, then their covariance is zero (i.e $\mathsf{Cov}[X_i, X_j] = \mathsf{V}_{ij} = 0$). However, the converse is not always true, if X_i and X_j have zero covariance, they need not be statistically independent.

A dimensionless measure which is a standardized version of the covariance is given by the correlation and denoted by r where

$$r_{ij} = \frac{\mathsf{V}_{ij}}{\sqrt{\mathsf{V}_{ii}}\sqrt{\mathsf{V}_{jj}}}. \tag{2.10}$$

Hence, it follows that the values of all the diagonal elements of the correlation matrix is 1. Random variables whose covariance is zero are called uncorrelated.

2.1.4 Partitioning the Mean Vector and Covariance Matrix

A random vector can be partitioned into two or more subsets, to distinguish the different types of variables. Consider a d-dimensional column random vector $\mathbf{X}$ that is partitioned into two groups of size m and $(d-m)$ respectively such that

$$\mathbf{X} = \left[\begin{array}{c} X_1 \\ \vdots \\ X_m \\ \hline X_{m+1} \\ \vdots \\ X_d \end{array}\right] = \left[\begin{array}{c} \mathbf{X}_\alpha \\ \hline \mathbf{X}_\beta \end{array}\right], \quad \text{and} \quad \boldsymbol{\mu} = \mathsf{E}(\mathbf{X}) = \left[\begin{array}{c} \mu_1 \\ \vdots \\ \mu_m \\ \hline \mu_{m+1} \\ \vdots \\ \mu_d \end{array}\right] = \left[\begin{array}{c} \boldsymbol{\mu}_\alpha \\ \hline \boldsymbol{\mu}_\beta \end{array}\right]. \tag{2.11}$$

It can be shown [26], that the covariance matrix is given by

$$\begin{aligned} \boldsymbol{\Sigma} &= \mathsf{E}\left[(\mathbf{X}-\boldsymbol{\mu})(\mathbf{X}-\boldsymbol{\mu})^T\right] \\ &= \left[\begin{array}{cc} \mathsf{E}(\mathbf{X}_\alpha-\boldsymbol{\mu}_\alpha)(\mathbf{X}_\alpha-\boldsymbol{\mu}_\alpha)^T & \mathsf{E}(\mathbf{X}_\alpha-\boldsymbol{\mu}_\alpha)(\mathbf{X}_\beta-\boldsymbol{\mu}_\beta)^T \\ \mathsf{E}(\mathbf{X}_\beta-\boldsymbol{\mu}_\beta)(\mathbf{X}_\alpha-\boldsymbol{\mu}_\alpha)^T & \mathsf{E}(\mathbf{X}_\beta-\boldsymbol{\mu}_\beta)(\mathbf{X}_\beta-\boldsymbol{\mu}_\beta)^T \end{array}\right] = \left[\begin{array}{c|c} \boldsymbol{\Sigma}_{\alpha\alpha} & \boldsymbol{\Sigma}_{\alpha\beta} \\ \hline \boldsymbol{\Sigma}_{\beta\alpha} & \boldsymbol{\Sigma}_{\beta\beta} \end{array}\right]. \end{aligned}$$

The covariance matrix of $\mathbf{X}_\alpha$ is given by $\boldsymbol{\Sigma}_{\alpha\alpha}$, that of $\mathbf{X}_\beta$ is given by $\boldsymbol{\Sigma}_{\beta\beta}$, and the covariance of elements from $\mathbf{X}_\alpha$ and $\mathbf{X}_\beta$ is given by $\boldsymbol{\Sigma}_{\alpha\beta}$, where $\boldsymbol{\Sigma}_{\alpha\beta} = \boldsymbol{\Sigma}_{\beta\alpha}^T$.

2.1.5 Uniform Distribution

A random variable X has a discrete uniform distribution if all the values that X attains (i.e., $x_1, x_2, \ldots, x_k$) are equally probable, hence $\text{Prob}(X = x_1) = \text{Prob}(X = x_2) = \cdots = \text{Prob}(X = x_k)$. However, a random variable X is said to have a continuous uniform distribution, if it attains a value x within a given interval with equal probability. For example, the uniform probability distribution function over the interval $a \leq x \leq b$ is given by

$$p(x) = \begin{cases} \frac{1}{b-a}, & \text{for } a \leq x \leq b; \\ 0, & \text{otherwise.} \end{cases} \tag{2.12}$$

The normalization condition for the pdf requires that $\int_a^b p(x)\mathrm{d}x = 1$. The concept of a uniformly distributed random variable is very important because it forms the basis of generating random numbers with more complicated distributions such as exponential, normal, etc.

2.1.6 Normal Distribution

The normal distribution is a unimodal bell shaped continuous probability distribution, where the individual data points are clustered around the mean. The normal distribution has a wide range of applicability, and is used throughout statistics due to the central limit theorem. The central limit theorem states that irrespective of the distribution of a set of independent random variables, provided that their variance is finite, the sum or average of them will be a random variable with a distribution close to a normal distribution [27].

The univariate normal distribution for random variable X, with mean μ and variance V, has a probability density function given by

$$p(x) = \frac{1}{\sqrt{2\pi\mathsf{V}}} \exp\left[\frac{-(x-\mu)^2}{2\mathsf{V}}\right] \quad \text{for} \quad x \in \mathbb{R}. \tag{2.13}$$

The univariate normal distribution is often denoted by $\mathcal{N}(\mu, \mathsf{V})$. The generalization of the univariate normal distribution to higher dimensions is known as the multivariate normal distribution. The d-dimensional normal distribution for random vector $\mathbf{X}$ is denoted by $\mathcal{N}_d(\boldsymbol{\mu}, \boldsymbol{\Sigma})$, and is given as shown in [26] by

$$p(\mathbf{x}) = \frac{1}{(2\pi)^{\frac{d}{2}} \det(\boldsymbol{\Sigma})^{\frac{1}{2}}} \exp\left[-\frac{1}{2}(\mathbf{x}-\boldsymbol{\mu})^T \boldsymbol{\Sigma}^{-1}(\mathbf{x}-\boldsymbol{\mu})\right] \quad \text{for} \quad \mathbf{x} \in \mathbb{R}^d. \tag{2.14}$$

2.2 Local Sensitivity Analysis

2.2.1 Propagation of Errors

The propagation of errors to the output of a model as a result of the uncertainties in the input of the model, and the numerical approximations used in the model, can be described by the “Error Propagation Equations”. The derivation of these equations are explained in detail in [23, 28]. Below we will make a brief review of the derivations.

Consider a model described by the following equation

$$Y = f(\mathbf{X}) = f(X_1, \ldots, X_d), \tag{2.15}$$

where Y is the model response or output which is dependent on parameters $\mathbf{X} = (X_1, \ldots, X_d)$. The parameters can be decomposed into nominal values $\boldsymbol{\mu} = (\mu_1, \ldots, \mu_d)$ which correspond to the expectations of the parameters, and their uncertainties $\delta\mathbf{X} = (\delta X_1, \ldots, \delta X_d)$ which correspond to their respective standard deviations.

Eq. (2.15) can then be rewritten as

$$Y = f(\mathbf{X}) = f(\boldsymbol{\mu} + \delta\mathbf{X}) = f(\mu_1 + \delta X_1, \ldots, \mu_d + \delta X_d). \tag{2.16}$$

Eq. (2.16) can be expanded in a Taylor series around the nominal values $\boldsymbol{\mu} = (\mu_1, \ldots, \mu_d)$ with variations $\delta X_i = (X_i - \mu_i)$ around μ_i. However, as stated in [23], for large complex systems, it is impractical to consider non-linear terms, hence a first order Taylor series expansion was considered, and Eq. (2.16) can now be rewritten as

$$Y = f(X_1, \ldots, X_d) \approx f(\boldsymbol{\mu}) + \sum_{i=1}^{d} \left(\frac{\partial Y}{\partial X_i}\right)_{\mu_i} \delta X_i. \tag{2.17}$$

The quantity $\left(\frac{\partial Y}{\partial X_i}\right)_{\mu_i}$ is defined as the sensitivity of the response Y to the parameter X_i, and is denoted by S_i. The d-dimensional sensitivity vector is denoted by S_Y with elements $[S_1 \ \cdots \ S_i \ \cdots \ S_d]^T$. It can be proved [23] that the uncertainty in the response or output of the model can be characterized by the variance which is given by

$$\mathsf{V}[Y] = S_Y^T \boldsymbol{\Sigma} S_Y. \tag{2.18}$$

Where $\boldsymbol{\Sigma}$ is the covariance matrix of the input variables.

2.2.2 Regression Based Methods

If an assumption is made that the input and output of the model are near linearly related, then regression based techniques such as the *standardized regression coefficient technique* and the *correlation coefficient technique* can be used as a measure of the sensitivity of the output to the input of the model [29]. Furthermore, if an assumption is made that the input and the output of the model are near monotonically related, then techniques such as the *standardized rank regression coefficient*, the *Spearman correlation* and the *partial rank correlation coefficients* can be used [30]. Regression based methods are not well suited for models that are non-linear and non-monotonic. The interested reader is referred to [31] for a review of regression based methods applied to sensitivity analysis.

2.2.3 Screening Methods and Experimental Designs

Screening methods are used to identify which input parameters have the largest influence on the output of a model. As stated in [23] the objective of screening methods is to arrive at a shortlist of important input parameters. One of the simplest class of screening methods is the classical One Factor At a Time (OFAT) method [32], where each parameter is varied one at a time to determine the response of the output to each individual parameter. Classical OFAT methods do not provide information about the response of the model to the interaction of two or more input parameters.

Experimental design [33] is a systematic approach to investigating a model by selecting combinations of input parameters in a structured way to highlight the relationship between the input and output of the model in the presence of parameter variation. One of the most popular experimental design methods is the factorial design [23]. Factorial design aims to capture the additive and interactive effects of two or more input parameters on the response of the model, and is often preferred to classical OFAT method. For a model with a large number of input parameters, considering all the possible interactions among the various parameters, can be computationally costly. By assuming that higher order interaction effects between the various input parameters are negligible, one can reduce the computational time. Methods such as Fractional Factorial Design (FFD) [34] are based on this assumption.

2.2.4 Reliability Methods

Sensitivity Analysis has also been used in cases where a system is to be designed so that the probability of failure does not exceed a certain threshold during a prescribed period. For such problems reliability methods are often used. Reliability methods often utilize statistical optimization algorithms [35] to seek the most likely "failure point" often referred to as the design point in the input parameter space. The probability of failure is then approximated by fitting a first or second order surface to the design point [23]. Most reliability methods often use the First Order Reliability Method (FORM) [35] and the Second order Reliability Method (SORM) [36, 37]. Recent advances in the field of reliability algorithms seeks to improve their efficiency by using techniques such as Advanced Mean Value methods (AMV) [38] and Two-point Adaptive Nonlinearity Approximation (TANA) based methods [39].

Reliability algorithms have been applied to a variety of problems such as nuclear safety [40] and structural safety [41, 42]. Despite the wide applicability of reliability algorithms, the results obtained must be treated with caution as these methods are susceptible to non-convergence or convergence to an erroneous design point particularly when the failure probability approaches the extreme values of 0 or 1, or when the design point is not unique [23].

2.2.5 Deterministic Methods

Local sensitivity indices can only be computed exactly by using deterministic methods [23]. Deterministic methods involves computing the rate of change of the output/response of the model to the input parameters at a certain base point in the input parameter space. These methods involve the derivatives (Jacobian) of the output of the model with respect to the input of the model. When the variations in the input parameters are small, perturbation theory [43] can be used in determining the sensitivity indices of the model.

Several deterministic methods exists for computing sensitivity indices, for a model with many outputs/responses and few input parameters, the Forward Sensitivity Analysis Procedure (FSAP) [22] can be used. However, most problems of practical applications involve few outputs/responses and many input parameters. For such problems, the Adjoint Sensitivity Analysis Procedure (ASAP) [22] is well suited for determining the sensitivity indices. Another deterministic method used in computing sensitivity indices for a model is the Green's function method [44]. However, this method is seldom used as it is computationally very expensive and difficult to implement. A detailed review of the different deterministic techniques is given in [23].

2.3 Global Sensitivity Analysis

2.3.1 Variance-Based Methods

These methods are based on the way that the variance in the output can be decomposed to the various variances due to the input factors and their interaction effects. The sensitivity index for variance-based methods is given as a ratio of the partial variance contributions of the input parameters of interest to the total variance of the output. A review of some variance-based methods, such as correlation ratio, Fourier Amplitude Sensitivity Test (FAST) and Sobol's method will be presented. The variance-based methods can be computationally expensive, however, as reported by Saltelli [2], the methods are well established, robust and model-independent. Other advantages of variance-based methods include their ability to take into account when computing sensitivity indices the interaction effects amongst the various input parameters and the ability to capture the full range of variation of each input parameter.

Correlation Ratio

Consider a model given by Eq. (2.15), where the input has a probability distribution function given by $p(\mathbf{x}) = p(x_1, \ldots, x_d)$. Consider the output Y to be a random variable which is dependent on the random vector $\mathbf{X}$ defined by its probability distribution function. The decomposition of the variance of the output is given by [45] as

$$\mathsf{V}(Y) = \mathsf{V}[\mathsf{E}(Y|X_i = x_i)] + \mathsf{E}[\mathsf{V}(Y|X_i = x_i)], \tag{2.19}$$

where the variance and expectation are denoted by V and E respectively. The first term on the right hand side of Eq. (2.19) is called the Variance Conditional Expectation (VCE) and the second term is the residual part. The VCE provides a measure of the importance that parameter x_i has on the output Y. Hence the *correlation ratio* [45]

$$\frac{\mathsf{V}[\mathsf{E}(Y|X_i = x_i)]}{\mathsf{V}(Y)}, \tag{2.20}$$

which describes the ratio of the VCE to the variance of the output is used as a measure of the sensitivity index. The correlation ratio has a value between 0 and 1, a value close to 0 implies that the input parameter under consideration is not important, while a value close to 1 implies that it is very important. For linear models, the correlation coefficients used in regression methods are equivalent to the correlation ratio. In practice, the correlation ratio can be determined by using latin hypercube sampling [46], a sampling scheme based on the "Importance Measure" of Hora and Iman [47] and a numerically robust numerical method [48] that involves the logarithmic scaling of the variances.

If we partition the input variables into two subsets such that

$$\mathbf{X} = (X_1, \ldots, X_d) = (\mathbf{X}_\alpha, \mathbf{X}_\beta). \tag{2.21}$$

We can describe two sensitivity indices for each subset; the first is known as the Main Sensitivity Index (MSI), which is given by

$$\text{MSI}_\alpha = \frac{V[\mathsf{E}(Y|\mathbf{X}_\alpha)]}{\mathsf{V}(Y)} = \frac{\mathsf{V}(Y) - \mathsf{E}[\mathsf{V}(Y|\mathbf{X}_\alpha)]}{\mathsf{V}(Y)}, \tag{2.22}$$

and this is interpreted as "*the relative amount of variance of Y that is expected to be removed if the true value(s) of the variable(s)* $\mathbf{X}_\alpha$ *becomes known*" [49]. Hence, this gives a measure of the contribution of the subset $\mathbf{X}_\alpha$ to the variance in the output. The second sensitivity index is known as the Total Sensitivity Index (TSI), which is given by

$$\text{TSI}_\alpha = \frac{\mathsf{E}[\mathsf{V}(Y|\mathbf{X}_\beta)]}{\mathsf{V}(Y)} = \frac{\mathsf{V}(Y) - \mathsf{V}[\mathsf{E}(Y|\mathbf{X}_\beta)]}{\mathsf{V}(Y)}, \tag{2.23}$$

and this is interpreted as "*the relative amount of variance of Y that is expected to remain if the true value of all other variables* $\mathbf{X}_\beta$ *becomes known*" [49]. Hence, this gives a measure of the contribution of the subset $\mathbf{X}_\alpha$ and all its interaction effects to the variance in the output. In subsequent sections we will discuss about the Fourier Amplitude Sensitivity Test (FAST) and the Sobol's method for determining sensitivity indices. For a single input parameter, the correlation ratio is equivalent to the main sensitivity index in the FAST and the Sobol's method.

Fourier Amplitude Sensitivity Test (FAST)

This is a sensitivity analysis method based on Fourier analysis. Consider a model given by Eq. (2.15), where the input has a probability distribution function given by $p(\mathbf{x}) = p(x_1, \ldots, x_d) = p_1(x_1) \cdots p_d(x_d)$, and the domain of the input is given by the unit hypercube $[0,1]^d$.

As shown in [50, 51] and explained further in [52], it is possible to use a multidimensional Fourier transform of the model to decompose the variance in the output as a function of their inputs and interaction effects. However, such an approach will be computationally expensive, hence a one-dimensional Fourier decomposition is done along a curve defined by a set of parametric equations that explores the space $[0,1]^d$. These parametric equations are given by

$$x_i(z) = G_i \sin(\omega_i z), \quad \text{for} \quad i = 1, 2, \ldots, d, \tag{2.24}$$

where $\{\omega_i\}$ is a set of integer angular frequencies, z is a scalar variable varying within the finite interval $(-\pi, \pi)$ and G_i's are optimal search curves, which are obtained as a solution of a set of differential equations [51]

$$\pi(1 - x_i^2)^{1/2} p_i(G_i) \frac{\mathrm{d}G_i(x_i)}{\mathrm{d}x_i} = 1, \tag{2.25}$$

with boundary conditions $G_i(0) = 0$. It can be shown [52] that the mean and variance of the output/response are given by

$$\mathsf{E}(y) = \frac{1}{2} \int_{-\pi}^{\pi} y(z) \mathrm{d}z, \tag{2.26}$$

and

$$\mathsf{V} = \mathsf{V}(y) \approx 2 \sum_{\omega=1}^{\infty} \left(A_\omega^2 + B_\omega^2 \right), \tag{2.27}$$

where $y(z) = y(G_1 \sin(\omega_1 z), \ldots, G_d \sin(\omega_d z))$ and the Fourier coefficients A_ω and B_ω are given by

$$A_\omega = \frac{1}{2} \int_{-\pi}^{\pi} y(z) \cos(\omega z) \mathrm{d}z, \tag{2.28}$$

$$B_\omega = \frac{1}{2} \int_{-\pi}^{\pi} y(z) \sin(\omega z) \mathrm{d}z. \tag{2.29}$$

As z varies for a given parameter x_i, all parameters change simultaneously along a curve that systematically explores the space $[0,1]^d$. The search curve becomes space filling, according to the ergodic theorem [53] if none of the frequency is obtainable as a linear combination of the others with integer coefficients [23]. The output variance arising from the uncertainty in the i^{th} input parameter is denoted by V_i and is obtained by evaluating the coefficients of A_ω and B_ω for the fundamental frequencies $\{\omega_i\}$ and its higher harmonics $j\omega_i$ for $j \in \mathbb{N}$.

$$\mathsf{V}_i = 2\sum_{j=1}^{+\infty}\left(A_{j\omega_i}^2 + B_{j\omega_i}^2\right). \tag{2.30}$$

The sensitivity index of the i^{th} input parameter quantifies the effect that the parameter has on the output and is denoted by

$$S_i = \frac{\mathsf{V}_i}{\mathsf{V}}. \tag{2.31}$$

An extension of the FAST Method is known as Extended FAST [52], this method allows for the determination of the total sensitivity index of a parameter. Whilst the FAST method is relatively cheaper than the Sobol's method in computing time [52], it is not sufficient if the sum of the first order indices (i.e. $S_1 + S_2 + \cdots + S_d$) is much less than 1 [9].

Sobol's Method

Consider a model given by Eq. (2.15), which is a square integrable function. The input variables are uncorrelated and uniformly distributed in the d-dimensional hypercube $[0,1]^d$. The Sobol's method [9] involves decomposing the function $f(\mathbf{x})$ into 2^d terms of increasing dimensionality:

$$f(\mathbf{x}) = f_\varnothing + \sum_{s=1}^{d}\sum_{i_1<\cdots<i_s}^{d} f_{i_1\cdots i_s}(x_{i_1},\ldots,x_{i_s}), \quad \text{where} \quad 1 \le i_1 < \cdots < i_s \le d. \tag{2.32}$$

Eq. (2.32) can be rewritten more explicitly as

$$f(\mathbf{x}) = f_\varnothing + \sum_{i=1}^{d} f_i(x_i) + \sum_{i=1}^{d}\sum_{j=i+1}^{d} f_{ij}(x_i,x_j) + \cdots + f_{12\cdots d}(x_1,\ldots,x_d), \tag{2.33}$$

where

$$f_\varnothing = \int f(\mathbf{x})\mathrm{d}\mathbf{x}. \tag{2.34}$$

For Eq. (2.32) to hold, the following properties must hold:

1. The zero means property

$$\int f_{i_1,\dots,i_s}(x_{i_1},\dots,x_{i_s})\mathrm{d}\mathbf{x}_k = 0 \quad \text{for} \quad k \in i_1,\dots,i_s; \tag{2.35}$$

2. The orthogonality property

$$\int f_{i_1,\dots,i_s}(x_{i_1},\dots,x_{i_s})f_{j_1,\dots,j_l}(x_{j_1},\dots,x_{j_l})\mathrm{d}\mathbf{x} = 0 \quad \text{for} \quad (i_1,\dots,i_s) \neq (j_1,\dots,j_l). \tag{2.36}$$

As shown in [9], by squaring Eq. (2.32) and integrating over the unit hypercube $[0,1]^d$ under conditions Eqs. (2.35) - (2.36) leads to

$$\int f^2(\mathbf{x})\mathrm{d}\mathbf{x} - f_\varnothing^2 = \sum_{s=1}^{d}\sum_{i_1<\cdots<i_s}^{d}\int f_{i_1\cdots i_s}^2(x_{i_1},\dots,x_{i_s})\mathrm{d}x_{i_1}\cdots\mathrm{d}x_{i_s}. \tag{2.37}$$

Let the variance of the function $f(\mathbf{x})$ be denoted by V, and the partial variances denoted by $\mathsf{V}_{i_1\cdots i_s}$. They are both given by

$$\mathsf{V} = \int f^2(\mathbf{x})\mathrm{d}\mathbf{x} - f_\varnothing^2 \quad \text{and} \quad \mathsf{V}_{i_1\cdots i_s} = \int f_{i_1\cdots i_s}^2(x_{i_1},\cdots,x_{i_s})\mathrm{d}x_{i_1}\cdots\mathrm{d}x_{i_s}.$$

Hence Eq. (2.37) can be rewritten as

$$\mathsf{V} = \sum_{s=1}^{d}\sum_{i_1<\cdots<i_s}^{d}\mathsf{V}_{i_1\cdots i_s}. \tag{2.38}$$

It expresses the variance in the output as summards of increasing dimensionality of the partial variances, and the sensitivity indices are defined as the ratio of the partial variances to the total variance, given mathematically as

$$S_{i_1\cdots i_s} = \frac{\mathsf{V}_{i_1\cdots i_s}}{\mathsf{V}}. \tag{2.39}$$

The formula above is similar to Eq. (2.22) for computing the main sensitivity index. The total sensitivity index for a subset of the input variables can also be obtained by using the Sobol's method as shown in [9], and this is similar to the total sensitivity index given in Eq. (2.23).

2.3.2 Entropy-Based Methods

These methods are based on the theory of information [54]. Consider a model given by Eq. (2.15) where the output uncertainty of a model is analysed in terms of Shannon's entropy [55]. The entropy-based method explained in [18], uses random perturbations of the input variables to create a randomized output Y with probability density $p(y)$. The probability density is approximated by a histogram, and the output is thus a discrete random variable with a corresponding entropy given by

$$H(Y) = -\sum_{y} p(y) \ln p(y), \tag{2.40}$$

with the convention $0 \ln 0 = 0$ [56]. Two other concepts that will be useful in the explanation of sensitivity indices are the conditional entropy and the mutual information. The conditional entropy $H(Y|X_i)$ provides a measure of uncertainty in the output if the input parameters X_i is known, and can be expressed mathematically as

$$H(Y|X_i) = \sum_{x} p(x) H(Y|X_i = x), \tag{2.41}$$

i.e. the uncertainty in the output Y is averaged over all possible values that the discrete random input variables X_i can attain. The mutual information $I(X_i; Y)$ is a quantity that measures the mutual dependence between the randomized input parameter X_i and the output Y and is expressed mathematically as

$$I(X_i; Y) = H(Y) - H(Y|X_i), \tag{2.42}$$

and it characterises the influence that X_i exerts on Y. The first order entropy sensitivity index is given by

$$S_i = \frac{I(X_i; Y)}{H(Y)}. \tag{2.43}$$

The sensitivity indices can also be obtained by using a relative entropy called the Kullback-Leibler entropy [57], rather than the Shannon entropy. A comparison of computational sensitivity indices by the the two entropy types is presented in [56]. The entropy-based methods have the capability of dealing with correlated input variables. They can also be used to determine the total sensitivity index of a subset of the input variables as shown in [18].

The entropy-based method provides a more general output variability than the variance-based methods when the distributions are non-symmetric and multi-modal [58]. However the entropy-based methods are not well established, requires the construction of conditional probability distributions, and are computationally very expensive. This makes the entropy-based method difficult to implement in practice. Moreover, entropy-based methods usually rank several variables around the same level due to its logarithm nature as reported in [56]. In reactor physics computations [13], groupwise neutron cross sections are described by only their first two moments, hence they are assumed to be normally distributed (i.e. unimodal and symmetric), and the variance-based methods provides a much more efficient way for determining sensitivity indices.

2.4 Application of Sensitivity Analysis to Reactor Physics

The uncertainties in the groupwise cross sections are expressed in terms of their covariance matrices. Computation of most nuclear reactor parameters are dependent on neutron cross sections. Hence lots of effort/research has been made over the past several years to improve the cross section files and their related uncertainty files. The uncertainty in the cross section is often propagated to the uncertainty in computed reactor parameters. The impact of uncertainty in the cross sections on reactor core calculations has been studied in [59, 60]. The interested reader is referred to a comprehensive annotated bibliography about generation and use of cross section covariance matrices written by Peelle [61].

Several groupwise cross section covariance matrices have been developed over the years, some of which are

1. ANL covariance matrix [5] which is based on educated guesses,
2. BOLNA covariance matrix [62] which is based on revised covariance data and is the joint effort of several laboratories,

3. NEA covariance matrix [13] as a 15-energy group cross section covariance matrix presenting a general overview of the presently available data.

The most up-to-date covariance library (at the time of writing this literature study) is the SCALE 6 covariance data [63], it has a total of 401 materials in the 44 energy group.

Most applications of sensitivity analysis to reactor physics have used local sensitivity analysis methods which are often based on perturbation theory [64]. The use of perturbation theory introduces the concept of adjoint flux, which is sometimes interpreted as an importance measure of the actual neutron flux. A historical overview of the application of perturbation theory in reactor physics, from the concept of adjoint flux, to the various developments in the field of perturbation theory is given in [4]. Using perturbation theory, the variation of any reactor parameter Q due to variations of groupwise neutron cross sections σ_j can be expressed according to [4] as

$$\frac{\delta Q}{Q} = \sum_j S_j \frac{\delta \sigma_j}{\sigma_j}, \tag{2.44}$$

where σ_j denotes a particular neutron groupwise cross section type in an energy group for a particular isotope of an element and S_j denotes the sensitivity indices which are given by

$$S_j = \frac{\partial Q}{\partial \sigma_j} \frac{\sigma_j}{Q}. \tag{2.45}$$

In some instances the dependence of the reactor parameter under consideration Q, is separated into those with an explicit dependence on cross sections and those with an implicit dependence on cross sections. This approach is used in the TSUNAMI[1] module of SCALE [65] which is developed at the Oak Ridge National Laboratory (ORNL). The reason for separating the dependence is because the cross section covariance matrices are supposed to be self shielded in the same way as cross sections, but this is rarely done, so the sensitivity indices are modified to include “implicit” effects which accounts for the impact of resonance self shielding [66]. Most sensitivity analysis calculations based on perturbation theory use diffusion theory, however, the results obtained can be doubtful, because of the limitations and approximations introduced in diffusion theory [3]. A method that uses perturbation theory to compute the sensitivity indices based on the transport theory is given by Takeda et al. [3]. Some codes that apply perturbation theory in computing sensitivity indices

[1]TSUNAMI: Tools for Sensitivity and Uncertainty Analysis Methodology Implementation

of reactor parameters are ERANOS (European Reactor ANalysis Optimized calculational System) [67], a Japanese Code SAGEP-T [3] and TSUNAMI [65]. The perturbation theory works well when the uncertainties are relatively small and for large input parameter uncertainties the polynomial chaos expansion can be used [68]. The polynomial chaos method has recently been successfully applied to assess the influence of data uncertainty on some parameters of interest (such as reflection and transmission coefficients) in neutron transport calculations [68]. However, this method is mathematically cumbersome, and so far works only for non-multiplying neutron systems.

Most applications of sensitivity analysis to reactor physics are based on local methods, the application of global sensitivity analysis to reactor physics has been limited. The major obstacles to the implementation of GSA as stated earlier are (a) the correlation between different input parameters and (b) the curse of the dimensionality, which is the exponential growth of computation cost with the number of input parameters. Most of the methods used for implementing global sensitivity analysis to reactor parameters are variance-based methods. Subsequently, we will present a brief review of the progress made so far in the scientific community in applying global sensitivity analysis to reactor physics.

Though not directly related to reactor physics, global sensitivity analysis methods have been used in environmental models to study the migration of radionuclides [7]. In [8] a variance-based GSA method which was an extension of the Sobol's method was developed. The aim was to determine the sensitivity indices when the input variables are functional such as stochastic processes or random spatial fields, as opposed to the Sobol's method that uses input scalar variables. This methodology was applied to determine the thermo-mechanical behaviour of fuel rods under irradiation by computing the fission gas swelling and the cladding creep. The functional inputs considered were modelled as Gaussian independent random variables and were initial internal pressure, pellet radius, cladding radius, microstructural grain diameter, fuel porosity and time dependent irradiation power.

A drawback of most of the variance based methods is the need for all input variables to be independent. Jacques et al. [6] developed a variance-based methodology for certain cases when the input variables of a model are correlated, and this methodology was applied in a study of nuclear reactor vessel dosimetry by computing the epithermal index for a given reactor. However, this methodology still needs further development, in particular when the model has many inputs.

An on-going project is the OECD-LWR-UAM[2] Benchmark [13], the objective of the project as stated in [13] is "*to determine the uncertainty in LWR system calculations at all stages of coupled reactor physics/thermal hydraulics calculations*". Using the one group neutron transport calculation available in MCNP[69], Puente-Espel et al. [70] considered only two elements, U-235 and Li-6, and determined their sensitivity indices for Exercise I-1 of the OECD LWR UAM benchmark. However, this methodology does not take the correlation between different energy groups of the groupwise neutron cross sections into account, and considering only two elements/materials fails to adequately take note of all the elements/materials given for Exercise I-1.

A methodology that utilizes groupwise neutron transport calculations, which is capable of dealing with correlations in the groupwise neutron cross sections and also capable of considering all the elements/materials required for the benchmark, would be preferable.

2.5 Higher Dimensional Integration Methods

The implementation of global sensitivity analysis often involves the integration of multidimensional integrals, where the dimensionality of the problem is dependent on the number of input parameters. Most computational approaches for evaluating numerical quadratures become computationally expensive or breakdown when the dimension becomes too high. We will discuss numerical schemes such as Monte Carlo, quasi-Monte Carlo and sparse grid quadratures that are capable of evaluating multidimensional integrals and they will be used in the computation of the global sensitivity indices.

2.5.1 Monte Carlo Integration

Monte Carlo integration is a sampling quadrature that utilizes random numbers to get random samples, the integral is then taken as an average of sampled random values. In practice the random numbers used are usually generated deterministically using random number generators. These random numbers generated are uniformly distributed in the range $0 \leq x < 1$ and are termed pseudo-random numbers. Some of the desirable properties of a good random number generator can

[2]OECD: Organization for Economic Co-operation and Development, LWR: Light Water Reactor, UAM: Uncertainty Analysis and Modelling

be found in [25, 71].

One of the main advantages of Monte Carlo over other integration techniques is that it provides an efficient way of evaluating integrals of high dimensions, thus helping to deal with the problem known as the curse of dimensionality. Consider the multi-dimensional integral given by

$$I = \int_0^1 \mathrm{d}x_1 \int_0^1 \mathrm{d}x_2 \cdots \int_0^1 \mathrm{d}x_d f(x_1, x_2, \ldots, x_d) \equiv \int_{[0,1]^d} f(\mathbf{x})\mathrm{d}\mathbf{x} \ , \tag{2.46}$$

where $\mathbf{x} = (x_1, x_2, \ldots, x_d)$ and $[0,1]^d$ is the unit hypercube. The strong law of large numbers [72] guarantees that for large N that

$$\lim_{N\to\infty} \frac{1}{N} \sum_{i=1}^{N} f(\mathbf{x}_i) = \mathsf{E}\left[f(\mathbf{x})\right], \tag{2.47}$$

hence an estimate for the integral can be given by

$$I \approx \frac{1}{N} \sum_{i=1}^{N} f(\mathbf{x}_i) = \mathsf{E}\left[f(\mathbf{x})\right]. \tag{2.48}$$

The formula above is valid for sufficiently large N, and it follows from the Central Limit Theorem that the distribution of I is almost normal, and the uncertainty associated with the quadrature is given in terms of the variance, and is expressed as

$$\mathsf{V}_I \approx \frac{1}{N}\mathsf{V}_f = \frac{1}{N}\mathsf{E}\left[\left[f(\mathbf{x}) - \mathsf{E}\left[f(\mathbf{x})\right]\right]^2\right] = \frac{1}{N}\left[\mathsf{E}\left[f^2(\mathbf{x})\right] - \left[\mathsf{E}\left[f(\mathbf{x})\right]\right]^2\right] \tag{2.49}$$

$$= \frac{1}{N}\left[\frac{1}{N}\sum_{1=1}^{N} f^2(\mathbf{x}_i) - \left[\frac{1}{N}\sum_{i=1}^{N} f(\mathbf{x}_i)\right]^2\right]. \tag{2.50}$$

From Eq. (2.49), we see that the uncertainty in the estimate of the integral, characterised by the standard deviation $\sqrt{\mathsf{V}_I}$, decreases as $N^{-\frac{1}{2}}$, which implies that to halve the uncertainty, four times as many samples are required.

The slow $N^{-\frac{1}{2}}$ convergence rate of the Monte Carlo method has led to different techniques to increase the accuracy for a given number of sample points. These techniques are known as reduction of variance. A summary of some important variance reduction techniques can be found in [72, 73]. A technique that is also used to improve the convergence rate to better than $N^{-\frac{1}{2}}$ is to use so-called *quasi-random numbers* instead of pseudo-random numbers in evaluation of the integral in

Eq. (2.46).

2.5.2 Quasi-Monte Carlo Integration

Quasi-Monte Carlo integration is very similar to the ordinary Monte Carlo Integration. The difference is, that instead of using pseudo-random numbers, quasi-random numbers are used. Quasi-random numbers are low discrepancy sequence of points that are designed deterministically to cover the hypercube as uniformly as possible by maximally avoiding each other to reduce gaps and the clustering of points [74]. There exist different kinds of quasi-random sequences such as Van der Corput, Halton, Faure, Sobol', Niederreiter, etc. An explanation and summary of these sequences can be found in [75, 76].

The convergence of the integral Eq. (2.46) using quasi-random numbers is given by $(\ln N)^d/N$ which is almost as fast as $1/N$. The main difficulty encountered when practically implementing quasi-Monte Carlo is that there is no straightforward method for estimating the accuracy achieved from the sampled values [77]. Most often randomization procedures are used as a basis for error estimation in quasi-Monte Carlo methods (see Subsection 4.1.1). Whilst both Monte Carlo and quasi-Monte Carlo integration techniques are robust and are not affected by the smoothness of the function being integrated, they have a relatively slow convergence rate. If the function to be integrated is continuous, smooth and differentiable, then an interpolatory quadrature such as sparse grids which exploits the smoothness of the function to increase the convergence rate can be used, to make a much more accurate estimate of the integral.

2.5.3 Sparse Grid

Consider a continuous and differentiable smooth function, for instance $f(x_1, x_2)$, then an interpolatory quadrature known as sparse grids that approximates $f(x_1, x_2)$ as a sum of monomials (powers of $\{x_1, x_2\}$) can be used to estimate the integral of the function. The sparse grid method is based on a combination of univariate quadrature rules that allow multidimensional integrals to be approximated with less function evaluations than the tensor product rule. For a q point d-dimensional product rule, the number of abscissas points required for evaluation increases exponentially with the dimension d and is given by q^d. However, the asymptotic accuracy of the product rule is determined by the highest *total degree* for which we can guarantee that all monomials will be integrated exactly [78].

The total degree of a monomial is the sum of all its exponents. As an example, consider an approximation to a two-dimensional function by using a product rule on the basis of two second-order polynomials $\{1, x_1, x_1^2\} \otimes \{1, x_2, x_2^2\} = \{1, x_1, x_2, x_1x_2, x_1^2, x_2^2, x_1^2x_2, x_1x_2^2, x_1^2x_2^2\}$. The monomials of total degree 2 are $\{x_1x_2, x_1^2, x_2^2\}$, similarly the monomials of total degree 3 are given by $\{\underline{x_1^3}, x_1^2x_2, x_1x_2^2, \underline{x_2^3}\}$, and lastly the monomials of total degree 4 are given by $\{\underline{x_1^4}, \underline{x_1^3x_2}, x_1^2x_2^2, \underline{x_1x_2^3}, \underline{x_2^4}\}$.

The monomials underlined are not contained in the set $\{1, x_1, x_2, x_1x_2, x_1^2, x_2^2, x_1^2x_2, x_1x_2^2, x_1^2x_2^2\}$, hence we cannot guarantee that monomials with a total degree of 3 or 4 will be integrated exactly. The asymptotic accuracy of the product rule is determined by all the monomials with a total degree of 2 or less, since 2 is the highest total degree for which we can guarantee that all monomials will be integrated exactly. Hence, when considering product rules, some monomials (such as $\{x_1^2x_2, x_1x_2^2, x_1^2x_2^2\}$ in this case) do not help to increase the asymptotic accuracy of the product grid and hence can be discarded without a loss of accuracy. In higher dimensions, the number of these unnecessary monomials increases rapidly which makes the product rule inefficient.

It is possible to get the same asymptotic accuracy of a product rule using a different rule that requires fewer points of the order of the relevant monomials. Smolyak [79] combined low order univariate product grids to yield "sparse grids" which is a small subset of points in the product grid and has the same asymptotic accuracy as a product grid. A more detailed mathematical discussion on the use of sparse grids to approximate multi-dimensional integrals is given in Appendix A.

As stated in [80] under certain smoothness conditions, piecewise linear interpolation in d-dimensional space on a sparse grid with N nodes, will have an order of interpolation error equal to $O(N^{-2}(\log N)^{(3d-1)})$ [81, 82], which is more efficient than using a full product grid where the error is of the order $O(N^{-\frac{2}{d}})$. Illustrative pictures showing sample points in two-dimensions for Monte Carlo, quasi-Monte Carlo and sparse grids are shown in Fig. 2.1. One can observe the clustering and gaps of the Monte Carlo sample points in Fig. 2.1a), the quasi-Monte Carlo sample points used in Fig. 2.1b) are much more uniform, with less gaps and clustering and Fig. 2.1c) illustrates sparse grid points which is a subset of a full product grid.

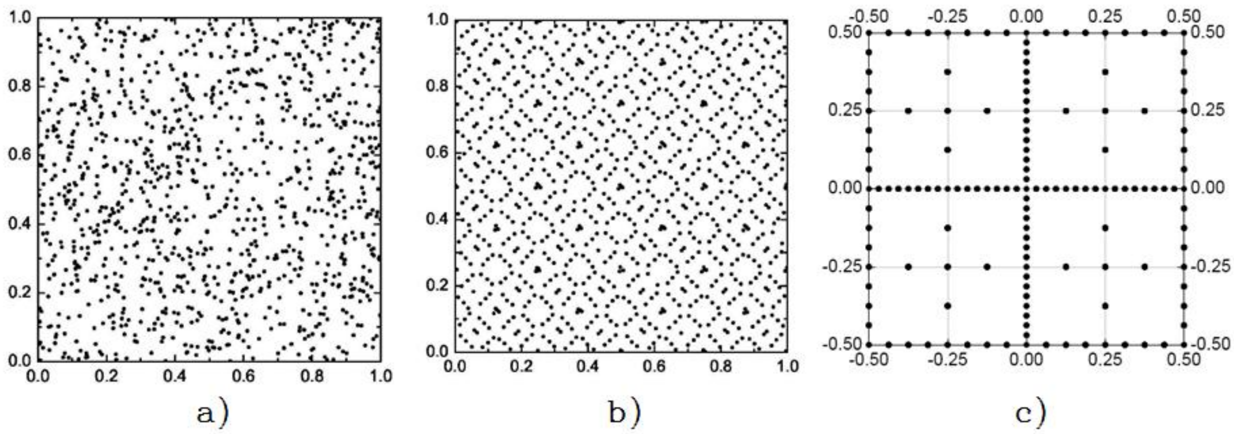

Figure 2.1: Illustrative picture of sample points in two-dimension used for (a) Monte Carlo (b) quasi-Monte Carlo and (c) sparse grid.

Chapter 3

Mathematical Formulation of Proposed GSA Methodology

Consider a problem in which some important reactor parameters, such as the neutron multiplication factors, the decay heat, etc., depend on groupwise neutron cross-sections. We will use Y to denote the reactor parameter of interest and X_i $(i = 1, 2, \ldots, d)$ to denote the cross-sections. The dependence of the parameter of interest on cross-sections can be written as a model similar to Eq. (2.15)

$$Y = f\left(X_1, X_2, \ldots, X_d\right), \tag{3.1}$$

where X_i are called inputs and Y is called the response or output of the model. The response of the model given in Eq. (3.1) is generally non-linear and is often calculated numerically in practice.

Subsequent sections in this chapter introduce the underlying mathematical basis for the proposed GSA methodology.

3.1 Functional ANOVA Decomposition for Independent Random Variables

Let $p(x_1, x_2, \ldots, x_d)$ be a joint probability distribution function of d random variables X_i:

$$P(\mathbf{x}) = \text{Prob}\left(X_1 \leq x_1, \ldots, X_d \leq x_d\right) = \int_{-\infty}^{x_1} \cdots \int_{-\infty}^{x_d} p\left(x_1, x_2, \ldots, x_d\right) \mathrm{d}x_1 \cdots \mathrm{d}x_d. \tag{3.2}$$

Let $f : \mathbb{R}^d \to \mathbb{R}$ be a square integrable function over $\mathbf{x} = (x_1, \ldots, x_d)$. The expected value and variance of the function $f(\mathbf{x})$ with respect to the probability density function $p(\mathbf{x})$ are defined as

$$\mathsf{E}\left[f(\mathbf{x})\right] = \int_{\mathbb{R}^d} f(\mathbf{x})\, p(\mathbf{x})\, \mathrm{d}\mathbf{x}, \quad \text{and} \quad \mathsf{V}\left[f(\mathbf{x})\right] = \int_{\mathbb{R}^d} \left(f(\mathbf{x}) - \mathsf{E}\left[f(\mathbf{x})\right]^2\right) p(\mathbf{x})\, \mathrm{d}\mathbf{x}. \tag{3.3}$$

The *functional ANOVA decomposition* is a representation of the function $f(\mathbf{x})$, as a sum of terms of increasing dimensionality as given by Eq. (2.32 - 2.33)

$$f(\mathbf{x}) = \sum_u f_u(\mathbf{x}_u) = f_\varnothing + \sum_i f_i(x_i) + \sum_{i<j} f_{ij}(x_i, x_j) + \cdots + f_{12\cdots d}(x_1, x_2, \ldots, x_d), \tag{3.4}$$

where the sum is assumed over 2^d subsets $u \subseteq \{1, 2, \ldots, d\}$ and $f_u(\mathbf{x}_u)$ is a function that depends on $\mathbf{x}$ only through x_i with $i \in u$. Here $\mathbf{X}_u$ is a subset of variables whose indices are in u, whereas $\mathbf{X}_{-u}$ are the variables with indices not in u and $|u|$ is the cardinality of the set u.

According to Sobol's definition, for the representation given by Eq. (3.4) to be a functional ANOVA decompositition it has to satisfy the so-called *zero means* and *orthogonality* properties [9, 83]. Let random variables X_i $(i = 1, 2, \ldots, d)$ be mutually independent with a joint probability density function $p(\mathbf{x}) = p_1(x_1)\, p_2(x_2) \cdots p_d(x_d)$. Using an analogy with the case of uniformly distributed input variables [9], one can demonstrate that the functional ANOVA can be constructed by applying the following recurrent formula

$$f_u(\mathbf{x}_u) = \int_{\mathbb{R}^{d-|u|}} \left(f(\mathbf{x}) - \sum_{v \subset u} f_v(\mathbf{x}_v)\right) p(\mathbf{x}_{-u})\, \mathrm{d}\mathbf{x}_{-u}. \tag{3.5}$$

The constant mean term, $f_\varnothing$, is thus obtained by calculating

$$f_\varnothing = \int_{\mathbb{R}^d} f(\mathbf{x}) p\left(\mathbf{x}\right) \mathrm{d}\mathbf{x}, \tag{3.6}$$

first order effects $f_i\left(x_i\right)$ $(i = 1, 2, \ldots, d)$ are obtained from

$$f_i\left(x_i\right) = \int_{\mathbb{R}^{(d-1)}} \left(f\left(\mathbf{x}\right) - f_\varnothing\right) \left[p\left(\mathbf{x}\right)/p\left(x_i\right)\right] \mathrm{d}\mathbf{x}/\mathrm{d}x_i \tag{3.7}$$

and so on. For functions $f_u\left(\mathbf{x}_u\right)$ obtained with recurrence Eq. (3.5), the zero means property becomes

$$\mathsf{E}\left[f_u\left(\mathbf{x}_u\right)\right] = \int_{\mathbb{R}^{|u|}} f_u\left(\mathbf{x}_u\right) p\left(\mathbf{x}_u\right) \mathrm{d}\mathbf{x}_u = \int_{\mathbb{R}^d} f_u\left(\mathbf{x}_u\right) p\left(\mathbf{x}\right) \mathrm{d}\mathbf{x} = 0. \tag{3.8}$$

The orthogonality property holds in the weighted form

$$\int_{\mathbb{R}^d} f_u(\mathbf{x}_u) f_v(\mathbf{x}_v) p(\mathbf{x}) \mathrm{d}\mathbf{x} = 0, \quad \text{for } u \neq v. \tag{3.9}$$

Eqs. (3.8 - 3.9) are crucial for the functional ANOVA method, because they lead to the variance decomposition formula

$$\mathsf{V}\left[f\left(\mathbf{x}\right)\right] = \sum_{u \subseteq \{1,2,\cdots,d\}} \mathsf{V}\left[f_u(\mathbf{x}_u)\right]. \tag{3.10}$$

Let us assume that the function $f\left(\mathbf{x}\right)$ allows order-wise decomposition over subsets of variables as shown in Eq. (3.4). Applying the variance operator Eq. (3.3) to the left-hand side and right-hand side of Eq. (3.4), and using a standard statistical formula we can write

$$\mathsf{V}\left[f(\mathbf{x})\right] = \mathsf{V}\left[\sum_u f_u(\mathbf{x}_u)\right] = \sum_u \mathsf{V}\left[f_u(\mathbf{x}_u)\right] + 2 \sum_{u, v \neq u} \mathsf{Cov}\left[f_u\left(\mathbf{x}_u\right), f_v\left(\mathbf{x}_v\right)\right]. \tag{3.11}$$

By definition,

$$\mathsf{Cov}\left[f_u\left(\mathbf{x}_u\right), f_v\left(\mathbf{x}_v\right)\right] = \int_{\mathbb{R}^d} \left(f_u\left(\mathbf{x}_u\right) - \mathsf{E}\left[f_u\left(\mathbf{x}_u\right)\right]\right) \left(f_v\left(\mathbf{x}_v\right) - \mathsf{E}\left[f_v\left(\mathbf{x}_v\right)\right]\right) p(\mathbf{x}) \mathrm{d}\mathbf{x} \tag{3.12}$$

and it can be observed from Eq. (3.12) that Eqs. (3.8 - 3.9) lead to the zero-covariance condition $\mathsf{Cov}\left[f_u\left(\mathbf{x}_u\right), f_v\left(\mathbf{x}_v\right)\right] = 0$ for $u \neq v$, and hence to the variance decomposition in the form of Eq. (3.10).

3.2 Global Sensitivity Analysis

The variance-based global sensitivity analysis method used in this study aims to quantify the relative importance of each input parameter in the response variance. It involves the calculation of the global sensitivity indices sometimes called Sobol's sensitivity indices [9, 83, 84].

In order to describe the global sensitivity indices let us introduce the following notations: $\mathcal{D} \equiv \{1, 2, \cdots, d\}$ will be used for the set of input variable indices and u for an arbitrary subset of $\mathcal{D}$. Hence, $\mathbf{X}_u$ is a subset of variables whose indices are in u, whereas $\mathbf{X}_{-u}$ are the complimentary variables, i.e. variables with indices not in u. Notation $|u|$ will be used for the cardinality of the set u. Variables X_i from non-overlapping sets u and $-u$ constitute the input vector, i.e. $\mathbf{X} = (\mathbf{X}_u, \mathbf{X}_{-u})^T$.

Sobol' [9, 83] introduced an alternative way of calculating sensitivity indices by sampling directly from $f(\mathbf{x})$, i.e. without passing through the ANOVA decomposition. Sobol's alternative formulae are valid for uniformly distributed, independent random variables. Consider a subset $\mathbf{X}_u$ of input variables, where $u \subset \mathcal{D}$, the Sobol's method can be generalized for continuous independent random variables with an arbitrary probability density function $p(\mathbf{x}) = p(x_1) \cdots p(x_d)$ as

$$f_\varnothing = \int_{\mathbb{R}^d} f(\mathbf{x})\, p(\mathbf{x})\, \mathrm{d}\mathbf{x}, \tag{3.13}$$

$$\mathsf{V} = \int_{\mathbb{R}^d} f^2(\mathbf{x})\, p(\mathbf{x})\, \mathrm{d}\mathbf{x} - f_\varnothing^2, \tag{3.14}$$

$$\mathsf{V}_{\mathbf{X}_u} = \int_{\mathbb{R}^{2d-|u|}} f(\mathbf{x})\, f(\mathbf{x}_u, \mathbf{x}'_{-u}) p(\mathbf{x})\, p\left(\mathbf{x}'_{-u}\right) \mathrm{d}\mathbf{x}\, \mathrm{d}\mathbf{x}'_{-u} - f_\varnothing^2, \tag{3.15}$$

$$\mathsf{V}^{\mathrm{tot}}_{\mathbf{X}_u} = \frac{1}{2} \int_{\mathbb{R}^{d+|u|}} \left[f(\mathbf{x}) - f(\mathbf{x}'_u, \mathbf{x}_{-u})\right]^2 p(\mathbf{x})\, p\left(\mathbf{x}'_u\right) \mathrm{d}\mathbf{x}\, \mathrm{d}\mathbf{x}'_u. \tag{3.16}$$

Here the prime symbol over a variable (e.g. as in $\mathbf{x}'_u$) means that this variable has to be sampled independently from the corresponding marginal distribution ($p(\mathbf{x}'_u)$ in this case) of its unprimed analogue. Using the results from Eqs. (3.13 - 3.16), the global sensitivity indices can be calculated as ratios

$$S^{\mathrm{tot}}_{\mathbf{X}_u} = \frac{\mathsf{V}^{\mathrm{tot}}_{\mathbf{X}_u}}{\mathsf{V}} \quad \text{and} \quad S_{\mathbf{X}_u} = \frac{\mathsf{V}_{\mathbf{X}_u}}{\mathsf{V}}, \tag{3.17}$$

where $S_{\mathbf{X}_u}$ is the main sensitivity index of subset $\mathbf{X}_u$, which gives a measure of the contribution of only subset $\mathbf{X}_u$ to the variance in the output. $S^{\text{tot}}_{\mathbf{X}_u}$ is the total sensitivity index of subset $\mathbf{X}_u$, which gives a measure of the contribution of subset $\mathbf{X}_u$ and all its interaction effects to the variance in the output. It should be noted that $f_\varnothing$ and V correspond to the output mean and the output variance.

The independence condition for input variables can be relaxed. As discussed in [6], it is not necessary that all variables are mutually independent (this result holds when assuming independent blocks of input variables $\mathbf{X}_\alpha$ instead of single independent input variables X_i). Thus, if subsets of variables from $\mathbf{X}_u$ and $\mathbf{X}_{-u}$ are mutually independent, i.e. $p(\mathbf{x}) = p(\mathbf{x}_u)\, p(\mathbf{x}_{-u})$, the sensitivity analysis formulas Eqs. (3.15 - 3.16) are still applicable. Moreover, as one can see from Eq. (3.14), the formula for the output variance does not explicitly involve any particular subset of input variables. As a result, the variance of the output V can be calculated with the method presented here even in the case when all input variables are correlated. Since the variance is used to characterise the uncertainty in the output due to the uncertainty of the input, this methodology can be used for uncertainty analysis disregarding whether normally distributed inputs are correlated or not.

As follows from the above description, the evaluation of sensitivity indices requires the calculation of the integrals in Eqs. (3.13 - 3.16), which can be written in the following general form

$$I_{d_{\text{eff}}}[g] = \int_{\mathbb{R}^{d_{\text{eff}}}} g(\tilde{\mathbf{x}})\, p(\tilde{\mathbf{x}}) \mathrm{d}\tilde{\mathbf{x}}, \tag{3.18}$$

where $I_{d_{\text{eff}}}[\cdot]$ is the integration operator, $g(\tilde{\mathbf{x}})$ represents a function being integrated, $d_{\text{eff}} = \dim(\tilde{\mathbf{x}})$ is the effective dimensionality of the integral and $p(\tilde{\mathbf{x}})$ is the joint probability density function of $\tilde{\mathbf{x}}$. For instance, in integral Eq. (3.15) function $g(\tilde{\mathbf{x}})$ represents $\left[f(\mathbf{x})\, f(\mathbf{x}_u, \mathbf{x}'_{-u}) - f^2_\varnothing\right]$, $\tilde{\mathbf{x}} = (\mathbf{x}, \mathbf{x}'_{-u}) = (\mathbf{x}_u, \mathbf{x}_{-u}, \mathbf{x}'_{-u})$, $p(\tilde{\mathbf{x}}) = p(\mathbf{x})\, p\left(\mathbf{x}'_{-u}\right)$ and the effective dimensionality is $d_{\text{eff}} = 2d - |u|$.

3.3 Block-Correlated Random Variables

From Section 2.1.4, we observe that if variables $\mathbf{X}_\alpha$ and $\mathbf{X}_\beta$ are independent, then $\mathbf{\Sigma}_{\alpha\beta} = \mathbf{\Sigma}_{\beta\alpha} = 0$ and the covariance matrix $\mathbf{\Sigma}$ becomes a block diagonal matrix

$$\mathbf{\Sigma} = \left(\begin{array}{c|c} \mathbf{\Sigma}_{\alpha\alpha} & 0 \\ \hline 0 & \mathbf{\Sigma}_{\beta\beta} \end{array}\right) = \operatorname{diag}\left(\mathbf{\Sigma}_{\alpha\alpha}, \mathbf{\Sigma}_{\beta\beta}\right) = \mathbf{\Sigma}_{\alpha\alpha} \oplus \mathbf{\Sigma}_{\beta\beta}, \tag{3.19}$$

where $\mathbf{\Sigma}_{\alpha\alpha} \oplus \mathbf{\Sigma}_{\beta\beta}$ denotes the direct sum of matrices $\mathbf{\Sigma}_{\alpha\alpha}$ and $\mathbf{\Sigma}_{\beta\beta}$. The same property holds for an arbitrary partitioning $\mathbf{X} = (\mathbf{X}_1, \mathbf{X}_2, \ldots, \mathbf{X}_\Gamma)$ of input variables to Γ mutually independent subsets

$$\mathbf{\Sigma} = \operatorname{diag}\left(\mathbf{\Sigma}_{11}, \mathbf{\Sigma}_{22}, \ldots, \mathbf{\Sigma}_{\Gamma\Gamma}\right) = \bigoplus_{\alpha=1}^{\Gamma} \mathbf{\Sigma}_{\alpha\alpha}. \tag{3.20}$$

The inverse of a block diagonal matrix is another block diagonal matrix, composed of the inverse of each block $\mathbf{\Sigma}^{-1} = \operatorname{diag}\left(\mathbf{\Sigma}_{11}^{-1}, \mathbf{\Sigma}_{22}^{-1}, \ldots, \mathbf{\Sigma}_{\Gamma\Gamma}^{-1}\right)$. Taking into account that for block matrices $\det(\mathbf{\Sigma}) = \prod_{\alpha=1}^{\Gamma} \det(\mathbf{\Sigma}_{\alpha\alpha})$, one can write the expression for the joint probability density function defined in Eq. (2.14) in a form that reflects the block-independence of variables as

$$p(\mathbf{x}) = \prod_{\alpha=1}^{\Gamma} p(\mathbf{x}_\alpha) = \prod_{\alpha=1}^{\Gamma} \frac{1}{(2\pi)^{\frac{d_\alpha}{2}} \det(\mathbf{\Sigma}_{\alpha\alpha})^{\frac{1}{2}}} \exp\left[-\frac{1}{2}\left(\mathbf{x}_\alpha - \boldsymbol{\mu}_\alpha\right)^T \mathbf{\Sigma}_{\alpha\alpha}^{-1} \left(\mathbf{x}_\alpha - \boldsymbol{\mu}_\alpha\right)\right], \tag{3.21}$$

where $p(\mathbf{x}_\alpha)$ is the joint probability density function of a subset α and $d_\alpha = \dim(\mathbf{x}_\alpha)$ is the number of variables in $\mathbf{X}_\alpha$.

3.4 Standard Normal Law Representation

The block-wise representation Eq. (3.21), of the joint probability density function Eq. (2.14) allows one to exploit the independence of different subsets of variables, however it gives no information about the practical way of a sensitivity index calculation. It is convenient to rewrite the expression in the so-called *standard* form in order to simplify future numerical evaluations of the global sensitivity indices.

Since covariance matrices are both symmetric and positive definite, for each $\mathbf{\Sigma}_{\alpha\alpha}$ there is a non-singular matrix $\mathbf{P}_\alpha$ such that $\mathbf{\Sigma}_{\alpha\alpha} = \mathbf{P}_\alpha \mathbf{P}_\alpha^T$ (Cholesky factorization). Consider the transformation

$\mathbf{z} = \mathbf{P}^{-1}(\mathbf{x} - \boldsymbol{\mu})$, where $\mathbf{P}^{-1} = \operatorname{diag}\left(\mathbf{P}_1^{-1}, \mathbf{P}_2^{-1}, \ldots, \mathbf{P}_\Gamma^{-1}\right)$. For any α it leads to

$$(\mathbf{x}_\alpha - \boldsymbol{\mu}_\alpha)^T \boldsymbol{\Sigma}_{\alpha\alpha}^{-1} (\mathbf{x}_\alpha - \boldsymbol{\mu}_\alpha) = \mathbf{z}_\alpha^T \mathbf{z}_\alpha, \tag{3.22}$$

and one can show that $\mathsf{E}[\mathbf{z}_\alpha] = 0$, $\mathsf{Cov}\left[\mathbf{z}_\alpha, \mathbf{z}_\alpha^T\right] = \mathbf{I}_\alpha$, where $\mathbf{I}_\alpha = \operatorname{diag}(1, 1, \ldots, 1)$ is the $d_\alpha \times d_\alpha$ identity matrix.

Taking into account the fact that $\mathsf{E}[\mathbf{x}_\alpha] = \boldsymbol{\mu}_\alpha$ one obtains

$$\mathsf{E}[\mathbf{z}_\alpha] = \mathsf{E}\left[\mathbf{P}_\alpha^{-1}(\mathbf{x}_\alpha - \boldsymbol{\mu}_\alpha)\right] = \mathbf{P}_\alpha^{-1}\mathsf{E}[(\mathbf{x}_\alpha - \boldsymbol{\mu}_\alpha)] = 0,$$

therefore

$$\begin{aligned}
\mathsf{Cov}\left[\mathbf{z}_\alpha, \mathbf{z}_\alpha^T\right] &= \mathsf{E}\left[\mathbf{z}_\alpha \mathbf{z}_\alpha^T\right] - \mathsf{E}[\mathbf{z}_\alpha]\,\mathsf{E}\left[\mathbf{z}_\alpha^T\right] = \mathsf{E}\left[\mathbf{z}_\alpha \mathbf{z}_\alpha^T\right] \\
&= \mathbf{P}_\alpha^{-1}\mathsf{E}\left[(\mathbf{x}_\alpha - \boldsymbol{\mu}_\alpha)(\mathbf{x}_\alpha - \boldsymbol{\mu}_\alpha)^T\right]\left(\mathbf{P}_\alpha^{-1}\right)^T \\
&= \mathbf{P}_\alpha^{-1}\boldsymbol{\Sigma}_{\alpha\alpha}\left(\mathbf{P}_\alpha^{-1}\right)^T = \mathbf{P}_\alpha^{-1}\mathbf{P}_\alpha\mathbf{P}_\alpha^T\left(\mathbf{P}_\alpha^{-1}\right)^T = \mathbf{I}_\alpha.
\end{aligned}$$

Since $\sum_{\alpha=1}^{\Gamma} \mathbf{z}_\alpha^T \mathbf{z}_\alpha = \mathbf{z}^T\mathbf{z}$, the joint probability density function can be written in the so-called standard form

$$p(\mathbf{z}) = \frac{1}{(2\pi)^{\frac{d}{2}}} \exp\left(-\frac{1}{2}\mathbf{z}^T\mathbf{z}\right) = \frac{1}{(2\pi)^{\frac{d}{2}}} \exp\left(-\frac{1}{2}\sum_{i=1}^{d} z_i^2\right), \tag{3.23}$$

where $p(\mathbf{x})\mathrm{d}\mathbf{x} = p(\mathbf{z})\mathrm{d}\mathbf{z}$. New standard random variables Z_i $(i = 1, 2, \ldots, d)$ have no physical meaning, they are uncorrelated with zero means and unit variances, i.e. $Z_i \sim \mathcal{N}(0, 1)$.

The representation of Eq. (3.23) can now be used for the calculation of sensitivity indices, variables Z_i can be sampled individually from $\mathcal{N}(0, 1)$ and the corresponding $\mathbf{x}$-points can be calculated as

$$\mathbf{x}(\mathbf{z}) = \boldsymbol{\mu} + \mathbf{P}\mathbf{z}. \tag{3.24}$$

Nevertheless, in order to simplify the sampling procedure, to allow the use of a single calculational path and to make a wider range of numerical integration techniques suitable for solving the problem, we do one more transformation from the normally distributed variables to the uniformly distributed ones.

For this, consider the following coordinate-wise change of variable from $z_i \in \mathbb{R}$ to $s_i \in (0,1)$:

$$s_i(z_i) = \Phi(z_i), \tag{3.25}$$

where $\Phi(\cdot)$ is the cumulative distribution function for the normal distribution. From the properties of $\Phi(\cdot)$, it follows that: $\lim_{z_i \to -\infty} s_i(z_i) = 0$, $\lim_{z_i \to +\infty} s_i(z_i) = 1$ and

$$\mathrm{d}s_i = \frac{1}{\sqrt{2\pi}} \exp\left(-\frac{1}{2} z_i^2\right) \mathrm{d}z_i. \tag{3.26}$$

Applying this transformation coordinate-wise (i.e. for $i = 1, 2, \ldots, d$), Eqs. (3.13 - 3.16) can be rewritten in terms of variables $\mathbf{s}$ as

$$f_\varnothing = \int_{(0,1)^d} f\left(\mathbf{x}[\mathbf{z}(\mathbf{s})]\right) \mathrm{d}\mathbf{s}, \tag{3.27}$$

$$\mathsf{V} = \int_{(0,1)^d} f^2\left(\mathbf{x}[\mathbf{z}(\mathbf{s})]\right) \mathrm{d}\mathbf{s} - f_\varnothing^2, \tag{3.28}$$

$$\mathsf{V}_{\mathbf{X}_u} = \int_{(0,1)^{2d-|u|}} f\left(\mathbf{x}[\mathbf{z}(\mathbf{s})]\right) f(\mathbf{x}_u[\mathbf{z}_u(\mathbf{s}_u)], \mathbf{x}'_{-u}[\mathbf{z}'_{-u}(\mathbf{s}'_{-u})]) \mathrm{d}\mathbf{s}\, \mathrm{d}\mathbf{s}'_{-u} - f_\varnothing^2, \tag{3.29}$$

$$\mathsf{V}_{\mathbf{X}_u}^{\mathrm{tot}} = \frac{1}{2} \int_{(0,1)^{d+|u|}} \left[f\left(\mathbf{x}[\mathbf{z}(\mathbf{s})]\right) - f(\mathbf{x}'_u[\mathbf{z}'_u(\mathbf{s}'_u)], \mathbf{x}_{-u}[\mathbf{z}_{-u}(\mathbf{s}_{-u})])\right]^2 \mathrm{d}\mathbf{s}\, \mathrm{d}\mathbf{s}'_u. \tag{3.30}$$

The representation of integrals in Eqs. (3.27 - 3.30) can be rewritten in a simpler and more general form similar to Eq. (3.18) as

$$I_{d_{\mathrm{eff}}}[g] = \int_{(0,1)^{d_{\mathrm{eff}}}} h(\tilde{\mathbf{s}}) \, \mathrm{d}\tilde{\mathbf{s}}, \tag{3.31}$$

where $h(\tilde{\mathbf{s}}) = g(\tilde{\mathbf{x}}[\tilde{\mathbf{z}}(\tilde{\mathbf{s}})])$. It should be noted that $z_i(s_i) = \Phi^{-1}(s_i)$ for $i = 1, 2, \ldots, d_{\mathrm{eff}}$ and $\Phi^{-1}(\cdot)$ is the inverse cumulative distribution function for the normal distribution, called the probit function.

Chapter 4

Implementation of Numerical Method and Results

4.1 Numerical Implementation

The integral in Eq. (3.31) can be approximated with a *quadrature* (sometimes called *cubature* in literature), that can be writen in the following general form

$$I_{d_{\text{eff}}}\left[g\left(\tilde{\mathbf{s}}\right)\right] \approx Q_{d_{\text{eff}}}^{N}\left[h\left(\tilde{\mathbf{s}}\right)\right] = \sum_{n=1}^{N} w_n h\left(\tilde{\mathbf{s}}_n\right), \tag{4.1}$$

where w_n are method-dependent quadrature weights, $h\left(\tilde{\mathbf{s}}_n\right)$ are samples of the integrand at method-dependent nodes $\tilde{\mathbf{s}}_n \in (0,1)^{d_{\text{eff}}}$ and N is the number of samples.

The integral in Eq. (3.31) is multidimensional and, therefore, special numerical techniques, that can cope with the curse of dimension are required to calculate it. Monte-Carlo, quasi-Monte Carlo and sparse grid integration methods are suitable for this task and will be considered in this study.

4.1.1 Monte Carlo and Quasi-Monte Carlo Quadratures

In the case of the Monte Carlo method the integral is sampled on a set of d_{eff}-dimensional *pseudo-random* points $\tilde{\mathbf{s}}_n$, uniformly distributed in the unit hypercube $(0,1)^{d_{\text{eff}}}$. In the case of quasi-Monte

Carlo, so-called *low discrepancy sequences* of *quasi-random* points (also uniformly distributed in $(0,1)^{d_{\mathrm{eff}}}$) are used for integration. For both Monte Carlo and quasi-Monte Carlo, the weights w_n are point-independent and equal, i.e. $w_n = 1/N$. The quasi-Monte Carlo quadratures have a higher asymptotic convergence rate and often outperform the Monte Carlo quadrature in practical applications [85].

There is a strong similarity between Monte Carlo and quasi-Monte Carlo quadratures except for the type of sampling points (pseudo-random or quasi-random) and the way of error estimation. The error estimation will be done in the same way for both quadratures (see the discussion below).

In this work we follow Sobol's recommendations [9] on the implementation of Monte Carlo and quasi-Monte Carlo quadratures for the calculation of sensitivity indices. In particular, sampling is done from hypercube $(0,1)^{2d}$ instead of $(0,1)^{d_{\mathrm{eff}}}$ and, in order to improve the accuracy in the estimation of variances from Eqs. (3.13 - 3.16), the function $f(\mathbf{x}) - c_0$ is evaluated instead of $f(\mathbf{x})$, where $c_0 \approx f_{\varnothing}$.

The usual method in Monte Carlo of estimating the integration error by using the sample variance, is not applicable for quasi-Monte Carlo. This is because the sample points are deterministic and hence correlated. Our estimation of the accuracy of the Monte Carlo and quasi-Monte Carlo quadratures in this study is based on a so-called randomization procedure [77]. This procedure consists of calculating R independent estimates, $\hat{I}_r^N$, of the integral in Eq. (3.31) by making $R-1$ random and uniformly distributed replications of the initial sequence.

Each new sequence of points is obtained from the initial one by a random modulo 1 shift. Let $\tilde{\mathbf{a}}$ be a sequence of pseudo or quasi-random points, we can create a randomized version of $\tilde{\mathbf{a}}$ corresponding to $\tilde{\mathbf{s}}$, where the replications of the initial sequence $\tilde{\mathbf{a}}$ is given by

$$\tilde{\mathbf{s}}_r = (\tilde{\mathbf{a}} + \tilde{\mathbf{u}}_r) \bmod 1 \quad \text{for} \quad r = 1, 2, \ldots, R-1. \tag{4.2}$$

$\tilde{\mathbf{u}}_r$ are independently distributed uniform random vectors and each replication $\tilde{\mathbf{s}}_r$, retains any special property the initial sequence $\tilde{\mathbf{a}}$ may have had.

The approximation to integral (3.31) is then calculated as an average of independent estimates, i.e.

$$\hat{I}^N = \frac{1}{R}\sum_{r=1}^{R} \hat{I}_r^N, \tag{4.3}$$

and the error of such an approximation is characterized by the sample standard deviation, defined as

$$\hat{\epsilon}_{RN} = \sqrt{\frac{1}{R\,(R-1)}\sum_{r=1}^{R}\left(\hat{I}_r^N - \hat{I}^N\right)^2}. \tag{4.4}$$

4.1.2 Sparse Grid Quadratures

A sparse grid $\mathcal{H}_{\ell,d_{\text{eff}}}$ is a set of d_{eff}-dimensional points, which is generated using the *Smolyak construction* [79] and is based on a chosen sequence of the univariate quadrature formulas Q_l, where $l \geq 0$ is the *accuracy level* of Q_l (see Appendix A for details). When applied to the integration of multivariate functions, the Smolyak construction is a multidimensional quadrature $Q_{\ell,d_{\text{eff}}}$ based on a tensor product of one-dimensional quadratures Q_l, which are combined in a special way in order to optimize the quadrature convergence rate [86, 87]. The sequence of univariate quadrature formulae Q_l leads to a sequence of sparse grid quadratures with an increasing *sparse grid accuracy level* $\ell \geq 0$.

$Q_{\ell,d_{\text{eff}}}\left[h\left(\tilde{\mathbf{s}}\right)\right]$ is a linear functional that depends on $h\left(\tilde{\mathbf{s}}\right)$ through function values at the set $\mathcal{H}_{\ell,d_{\text{eff}}}$ and the number of terms N in Eq. (4.1) is defined by its cardinality. The sparse grid points $\tilde{\mathbf{s}}_n \in \mathcal{H}_{\ell,d_{\text{eff}}}$ and the quadrature weights w_n can be calculated using the procedure described in Appendix A.

If $\mathcal{H}_{\ell,d_{\text{eff}}} \subset \mathcal{H}_{\ell+1,d_{\text{eff}}}$ the quadrature is called *nested.* Nested quadratures permit the use of function values from previous levels, thus making integration less computationally expensive. Quadrature rules are said to be *open* when they do not include points on the boundary and *closed* otherwise. Points on the boundary (i.e. $s_i = 0$ or $s_i = 1$ for $i = 1, 2, \ldots, d_{\text{eff}}$) represent a problem for the numerical integration in Eq. (3.31), as a transformation $s_i \rightarrow z_i$ will lead to infinities in these points. Hence, only nested and strictly open sparse grid quadratures will be used in this work.

The sequence of sparse grid quadratures naturally leads to a formula for a practical estimation of the integration error

$$\hat{\epsilon}_\ell = \left|Q_{\ell,\,d_{\text{eff}}}\left[h\left(\tilde{\mathbf{s}}\right)\right] - Q_{\ell-1,\,d_{\text{eff}}}\left[h\left(\tilde{\mathbf{s}}\right)\right]\right|, \tag{4.5}$$

although this estimation is usually quite conservative.

Note that sparse grids are often defined on the hypercube $s^* \in [-1, 1]^{d_{\text{eff}}}$. In this case they can easily be mapped to the unit hypercube $[0, 1]^{d_{\text{eff}}}$ using the transformation of variables $s_i = (s_i^* + 1)/2$. When this mapping is performed, all sparse grid quadrature weights w_n have to be adjusted by a factor of $2^{d_{\text{eff}}}$.

4.1.3 Inversion of the Standard Normal Cumulative Density Function

According to the methodology discussed in Section 3.4, each sample vector $\tilde{\mathbf{s}}_n$, generated with either Monte Carlo, quasi-Monte Carlo or sparse grid techniques, requires transformation to the corresponding $\tilde{\mathbf{z}}_n$-vector. The traditional way to generate normally distributed points in conventional Monte Carlo, is to sample from the uniform distribution and then to use the so-called Box-Muller transformation [88]. Unfortunately it is not recommended [75] for use with quasi-Monte Carlo and is not suitable for use with sparse grids. An alternative way is to sample from the uniform distribution and then to use the inverse of the standard normal cumulative density function. It is recommended to use Moro's inversion algorithm [89], which is reported to be faster than the Box-Muller approach and has good accuracy for both the central region and the tails of the normal distribution [75]. In our work, Moro's algorithm is used for variable transformation $\tilde{\mathbf{s}}_n \to \tilde{\mathbf{z}}_n$ $(n = 1, 2, \ldots, N)$ coordinate-wise (i.e. for each $s_{i,n}$, where $i = 1, 2, \ldots, d_{\text{eff}}$) for Monte Carlo, quasi-Monte Carlo and sparse grid samples.

4.1.4 Algorithm for Calculation of Global Sensitivity Indices

An algorithm was written to illustrate all the steps in the calulational path used to compute global sensitivity indices based on Monte Carlo, quasi-Monte Carlo and sparse grid quadratures. Note that this algorithm is given for the sake of illustration and do not contain details about possible memory management or performance enhancements.

1. Inputs required for the computation of global sensitivity indices.

   $\boldsymbol{\mu}_1, \boldsymbol{\mu}_2, \ldots, \boldsymbol{\mu}_\Gamma$ - partitioned mean vectors.

   $\boldsymbol{\Sigma}_{11}, \boldsymbol{\Sigma}_{22}, \ldots, \boldsymbol{\Sigma}_{\Gamma\Gamma}$ - corresponding covariance matrices.

Level_max - maximum level to be used by sparse grids.

N - number of MC and qMC samples to be used.

R - used for the randomization procedure in MC and qMC.

2. Create a mean vector $\boldsymbol{\mu}$ for the problem by combining the partitioned mean vectors

   $\boldsymbol{\mu} = (\boldsymbol{\mu}_1, \boldsymbol{\mu}_2, \ldots, \boldsymbol{\mu}_\Gamma)$, where cardinality of $\boldsymbol{\mu}$ is d.

3. Perform Cholesky decomposition for each corresponding covariance matrix in step 1.

   $\boldsymbol{\Sigma}_{\alpha\alpha} = \mathbf{P}_\alpha \mathbf{P}_\alpha^* \quad \text{for } \alpha = 1 \text{ to } \Gamma.$

4. Take the direct sum of all the corresponding Cholesky decomposed matrices in step 3 to define the Cholesky decomposed matrix for the problem given by $\mathbf{P}$, i.e.:

   $\mathbf{P} = \bigoplus_{\alpha=1}^{\Gamma} \mathbf{P}_\alpha.$

5. Sample $2d$ vector,

   $(s_1, \ldots, s_d, s_{d+1}, \ldots, s_{2d})$,

   define vectors $\mathbf{s}$ and $\mathbf{s}'$ as

   $\mathbf{s} = (s_1, \ldots, s_d)$ and $\mathbf{s}' = (s_{d+1}, \ldots, s_{2d}) = (s'_1, \ldots, s'_d)$.

   Note that both $\mathbf{s}$ and $\mathbf{s}' \in [0, 1)^d$.

   - **For Monte Carlo**

     Generate $2d$ pseudo-random vector.

   - **For quasi-Monte Carlo**

     Generate $2d$ quasi-random vector.

   - **For sparse grids**

     For preferred rule and specific level ℓ generate sequence of $2d$ points for sparse grids.

6. Use Moro's inversion to convert $\mathbf{s}$ and $\mathbf{s}'$ to normally distributed vectors,

   $\mathbf{z} = \Phi^{-1}(\mathbf{s})$ and $\mathbf{z}' = \Phi^{-1}(\mathbf{s}')$.

7. Define random vectors $\mathbf{X}$ and $\mathbf{X}'$,

   $\mathbf{X} = \boldsymbol{\mu} + \mathbf{P}\mathbf{z}$ and $\mathbf{X}' = \boldsymbol{\mu} + \mathbf{P}\mathbf{z}'$.

8. Define subset of variables of interest $\mathbf{X}_u$, (i.e. cross sections of interest)

   $\mathbf{X} = (\mathbf{X}_u, \mathbf{X}_{-u})^T$ and $\mathbf{X}' = (\mathbf{X}'_u, \mathbf{X}'_{-u})^T$,

   where $\mathbf{X}_{-u}$ are the complimentary variables.

9. Substitute $\mathbf{X}$ and $\mathbf{X}'$ in Eqs. (3.27 - 3.30).

10. Compute the main and total sensitivity indices with the aid of Eq. (3.17).

    For Monte Carlo and quasi-Monte Carlo

11. Repeat steps 5 to 10, $N - 1$ times.

12. Get estimates for $f_\varnothing, \mathsf{V}, S_{\mathbf{X}_u}$ and $S^{\text{tot}}_{\mathbf{X}_u}$

    each estimate $\hat{I}_r^N$ was obtained as an average of N sampled values

    $\hat{I}_r^N = \frac{1}{N} \sum_{i=1}^{N} \hat{I}_{i,r}$.

13. Repeat steps 5 to 12, $R - 1$ times, where each new sequence of points ($\mathbf{s}$ and $\mathbf{s}'$) are obtained from the initial one by a random modulo 1 shift.

    The average values of $f_\varnothing, \mathsf{V}, S_{\mathbf{X}_u}$ and $S^{\text{tot}}_{\mathbf{X}_u}$ along with their quadrature error is determined.

    The average value $\hat{I}^N$ is given by $\hat{I}^N = \frac{1}{R} \sum_{r=1}^{R} \hat{I}_r^N$ and the associated quadrature error is given by Eq. (4.4).

    For Sparse grids

14. For level $\ell = 1$ to Level_max, repeat steps 5 to 10,

    evaluate $f_\varnothing, \mathsf{V}, S_{\mathbf{X}_u}$ and $S^{\text{tot}}_{\mathbf{X}_u}$ and get the associated quadrature error given by Eq. (4.5).

4.2 Results

A Fortran program was written to implement all the steps of the methodology outlined in Chapter 3. The program was subdivided into blocks of code, where each block had an input to be evaluated to give an expected output, and corresponded to step(s) along the calculational path of the methodology. The testing, verification and validation of the program was done for each block of code using test functions, for which the corresponding results could be evaluated analytically. Several test functions were used and an analysis of the accuracy, convergence and stability of the results were performed. In subsequent subsections we will present an example of such a test function, and an application of the methodology presented in Chapter 3 to nuclear reactor calculations. In implementing Monte Carlo, pseudo-random points were generated using the Fortran intrinsic subroutine `random_number()` and a Sobol' quasi-random number generator written by John Burkardt [90] was used for implementing quasi-Monte Carlo. The Sobol' quasi-random sequence was chosen because of its superior convergence when compared to other low discrepancy sequences as reported in [91]. Furthermore, a randomization procedure Eq. (4.4) was used in estimating the integration error, $\hat{\epsilon}_{RN}$, for both Monte-Carlo and quasi-Monte Carlo quadratures. The implementation of sparse grid quadratures was greatly facilitated by subroutines written by John Burkardt [90]. Different open sparse grid quadrature rules such as Fejer [92], Gauss-Patterson and Gauss-Legendre rules [93] were applied (note that closed rules were also tested and, as expected, numerical problems for the boundary points were encountered). Furthermore, a conservative procedure defined by Eq. (4.5) was used in estimating the integration error $\hat{\epsilon}_{\ell}$ for the sparse grid quadrature.

4.2.1 Example

This subsection intends to use an example to illustrate the accuracy of the sensitivity indices results obtained by the Fortran program. This was part of the verification procedure of the Fortran program written for this mini-dissertation. A simple test function $f : \mathbb{R}^4 \to \mathbb{R}$ defined as

$$f(\mathbf{x}) = {x_1}^2 + x_1{x_3}^4 + {x_2}^3{x_4}^2 + x_1x_2x_4, \tag{4.6}$$

for which the sensitivity indices of interest can be evaluated with the aid of a commercial software package such as Mathematica® was chosen. The input vector $\mathbf{x} = (x_1\ x_2\ x_3\ x_4)^T$ is normally distributed, with the expectation and covariance matrix given by $\boldsymbol{\mu}$ and $\boldsymbol{\Sigma}$ respectively, where

$$\boldsymbol{\mu} = \left[\begin{array}{c} 5.11 \\ 10.24 \\ \hline 7.35 \\ 14.38 \end{array}\right] \quad \text{and} \quad \boldsymbol{\Sigma} = \left[\begin{array}{cc|cc} 3.20 & 1.72 & 0.00 & 0.00 \\ 1.72 & 2.48 & 0.00 & 0.00 \\ \hline 0.00 & 0.00 & 5.61 & 2.32 \\ 0.00 & 0.00 & 2.32 & 8.40 \end{array}\right]. \tag{4.7}$$

From Eq. (4.7), we can observe that the input vector has been partitioned into two independent subsets.

Let $u = \{x_1, x_2\}$ be the subset of input variables of interest, the partitioned vector corresponding to this subset is given by $\mathbf{X}_u = (x_1\ x_2)^T$. Using Eqs. (3.13 - 3.17) the main and total sensitivity index of $\mathbf{X}_u$ were obtained with the aid of Mathematica®, and these are considered to be the reference results, which are reported in Table 4.1. The reference sensitivity indices results are compared to those evaluated numerically with the Fortran program, which are reported in Tables 4.2 and 4.3, and the relative absolute error denoted by RAE is used as a basis for the comparison of the results. The relative absolute error in this context is defined mathematically as

$$\text{RAE} = \frac{|\text{computed value} - \text{reference value}|}{|\text{reference value}|} \times 100\ [\%], \tag{4.8}$$

where the computed value is the sensitivity index obtained from the Fortran program and the reference value is the sensitivity index obtained from Mathematica®.

Table 4.1: Reference results for sensitivity indices obtained with the aid of Mathematica®.

	$\text{S}_{\mathbf{X}_u}$	$\text{S}^{\text{tot}}_{\mathbf{X}_u}$
Mathematica®	4.9308×10^{-1}	5.7113×10^{-1}

Table 4.2: Monte Carlo and quasi-Monte Carlo sensitivity indices results for $R = 100$ and $N = 10^6$.

	$\text{S}_{\mathbf{X}_u}$	RAE of $\text{S}_{\mathbf{X}_u}(\%)$	$\text{S}^{\text{tot}}_{\mathbf{X}_u}$	RAE of $\text{S}^{\text{tot}}_{\mathbf{X}_u}(\%)$
Monte Carlo	4.9317×10^{-1}	1.8×10^{-2}	5.7143×10^{-1}	5.3×10^{-2}
Quasi-Monte Carlo	4.9309×10^{-1}	2.0×10^{-3}	5.7114×10^{-1}	1.8×10^{-3}

Ideally the number of decimal places or significant figures that a result is to be reported is determined by its uncertainty, however in Tables 4.1 - 4.3 the results for sensitivity indices were reported to 5 decimal places in scientific notation. This is because at least 5 decimal places were needed to show the difference between results of sensitivity indices computed by different methods. The

Table 4.3: Sparse grids sensitivity indices results for level $\ell = 4$.

	Sampling points	$S_{\mathbf{X}_u}$	RAE of $S_{\mathbf{X}_u}$(%)	$S^{\text{tot}}_{\mathbf{X}_u}$	RAE of $S^{\text{tot}}_{\mathbf{X}_u}$(%)
Fejer-Type 1	6401	4.9455×10^{-1}	3.0×10^{-1}	5.6637×10^{-1}	8.3×10^{-1}
Fejer-Type 2	6401	4.9416×10^{-1}	2.2×10^{-1}	5.7030×10^{-1}	1.5×10^{-1}
Gauss-Patterson	6401	4.9333×10^{-1}	5.1×10^{-2}	5.7075×10^{-1}	6.6×10^{-2}
Gauss-Legendre	9377	4.9372×10^{-1}	1.3×10^{-1}	5.7070×10^{-1}	7.5×10^{-2}

results for the relative absolute error were reported to 2 significant figures in scientific notation. From Tables 4.2 and 4.3, one can observe that the results of sensitivity indices obtained from the Fortran program are in good agreement with those obtained from Mathematica® in Table 4.1, and the relative absolute error for all the sensitivity indices computed in Tables 4.2 and 4.3 is below 1%. It should be noted that the accuracy of the computed sensitivity indices can be improved further by increasing the number of samples for Monte Carlo and quasi-Monte Carlo, or by increasing the level for sparse grids.

4.2.2 Application to Nuclear Reactor Calculations

The methodology presented in Chapter 3 was applied to nuclear reactor calculations. The reactor parameter of interest is the infinite neutron multiplication factor, k_∞, and the influence of the 2-group cross-sections uncertainty on the uncertainty in k_∞ is studied with the aid of global sensitivity analysis. To illustrate the methodology, two cases were considered: one with a diagonal covariance matrix and another one with a block-diagonal covariance matrix.

In the first case (hereafter referred to as Case A), assembly homogenized 2-group data for the Peach Bottom boiling water reactor, as given in Table 4.4, with an energy boundary of 0.625 eV was used [94]. The neutron cross-sections in Case A were assumed to be independent and normally distributed, and their mean values (given in the third column of Table 4.4,) correspond to the vector $\boldsymbol{\mu}$ used in the methodology. The percentage relative standard deviations (fourth column of Table 4.4) correspond to the square root of the variances, which are the diagonal terms of the neutron cross-section covariance matrix. Note, that the terms D_1 and D_2 from Table 4.4 describe leakage, and are not needed when computing the infinite neutron multiplication factor, hence they are not used in this study. Taking the above mentioned conditions into account, the 2-group infinite neutron multiplication factor was modelled as [95]

$$k_\infty = \frac{\nu\Sigma_f^1}{\Sigma_c^1 + \Sigma_f^1 + \Sigma_s^{1\to2}} + \frac{\nu\Sigma_f^2\Sigma_s^{1\to2}}{\left(\Sigma_c^2 + \Sigma_f^2\right)\left(\Sigma_c^1 + \Sigma_f^1 + \Sigma_s^{1\to2}\right)}, \tag{4.9}$$

where the traditional notation for macroscopic cross-sections, as given in Table 4.4, were used.

Table 4.4: Assembly homogenized 2-group data [94].

Variable	Abbreviation	Value	% Std dev
Fast capture, cm^{-1}	Σ_c^1	5.336×10^{-3}	1.208
Thermal capture, cm^{-1}	Σ_c^2	2.693×10^{-2}	0.543
Fast fission, cm^{-1}	Σ_f^1	1.9124×10^{-3}	0.681
Thermal fission, cm^{-1}	Σ_f^2	2.8438×10^{-2}	0.323
Fast neutron production, cm^{-1}	$\nu\Sigma_f^1$	4.920×10^{-3}	0.977
Thermal neutron production, cm^{-1}	$\nu\Sigma_f^2$	6.929×10^{-2}	0.448
Fast diffusion coefficient, cm	D_1	5.9530×10^{-1}	0.885
Thermal diffusion coefficient, cm	D_2	2.2140×10^{-1}	0.139
Fast removal, cm^{-1}	$\Sigma_s^{1\to2}$	2.063×10^{-2}	1.114

In the second case (hereafter referred to as Case B), we assumed a test block-diagonal covariance matrix. A test matrix is artificially constructed based on the 2-group covariance matrix from [94] in such a way that the input variables can be partitioned into three mutually independent subsets $\{\Sigma_c^1, \Sigma_c^2, \Sigma_f^1, \Sigma_f^2\}$, $\{\nu\Sigma_f^1, \nu\Sigma_f^2\}$ and $\{\Sigma_s^{1\to2}\}$. The partitioned vectors corresponding to this subsets are given respectively by $\mathbf{X}_u = (\Sigma_c^1\ \Sigma_c^2\ \Sigma_f^1\ \Sigma_f^2)^T$, $\mathbf{X}_u = (\nu\Sigma_f^1\ \nu\Sigma_f^2)^T$ and $\mathbf{X}_u = (\Sigma_s^{1\to2})$ The block correlated covariance matrix is given in Table 4.5, where the diagonal terms are the percentage relative standard deviation and the off-diagonal terms are the correlation coefficients. It should be noted that the elements of the first subset correspond to those terms that contribute to the absorption cross-section. The elements of the second subset correspond to those terms that contribute to the production of neutrons, and the last subset corresponds to the removal of neutrons from the fast group to the thermal group. The mean values of the cross-sections are the same as in the previous case, i.e. as given in the third column of Table 4.4.

Table 4.5: Test covariance matrix.

	Σ_c^1	Σ_c^2	Σ_f^1	Σ_f^2	$\nu\Sigma_f^1$	$\nu\Sigma_f^2$	$\Sigma_s^{1\to 2}$
Σ_c^1	1.21	0.23	-0.63	-0.04	0	0	0
Σ_c^2	0.23	0.54	-0.09	-0.48	0	0	0
Σ_f^1	-0.63	-0.09	0.68	0.11	0	0	0
Σ_f^2	-0.04	-0.48	0.11	0.32	0	0	0
$\nu\Sigma_f^1$	0	0	0	0	0.98	0.12	0
$\nu\Sigma_f^2$	0	0	0	0	0.12	0.45	0
$\Sigma_s^{1\to 2}$	0	0	0	0	0	0	1.11

It should be emphasised that neither example considered pretends to reflect physical reality, but both the cross-section values and the elements of the test covariance matrix are of a realistic order of magnitude (close to the values given in [94]), hence this example is representative and suitable for the testing of the method. The results and conclusions will therefore be given in order to characterise the method presented and not the neutron multiplication properties of the Peach Bottom BWR.

Different open sparse grid quadratures were applied to both cases, however the Gauss-Legendre quadrature outperformed the other rules in terms of computational time needed to achieve a given accuracy for the cases considered, and its results will be reported up to a sparse grid level of $\ell = 4$. The implementation of Monte Carlo and quasi-Monte Carlo quadrature were done by considering $R = 100$ independent sequences and $N = 10^6$ samples in each sequence.

Variations were introduced into the neutron cross-sections by using a standardizing transformation as explained in Eq. (3.24), i.e. $\mathbf{x}(\mathbf{z}) = \boldsymbol{\mu} + \mathbf{P}\mathbf{z}$, where $\mathbf{P}$ is the Cholesky decomposed neutron cross-section covariance matrix, and $\mathbf{z}$ is obtained by using Moro's inversion of samples required by each of the implemented quadratures. Finally, in order to improve the accuracy of the Monte Carlo estimation of integral Eq. (3.31), a variance reduction technique [9], which consists of sampling function $f(\mathbf{x}) - c_0$ instead of $f(\mathbf{x})$ in Eqs. (3.13 - 3.16), where $c_0 \approx f_\varnothing$ was used.

The computed sensitivity indices for each of the variables in Case A are given in Table 4.6, and the computed sensitivity indices for each subset in Case B are given in Table 4.7. The computed values of the sensitivity indices reported on in Tables 4.6 and 4.7 are multiplied by a factor 100 in order to improve readability (we do not use % in reporting the sensitivity indices, in order to avoid confusion with the relative quadrature error that will be given in % and is reported on in other tables).

Table 4.6: Sensitivity indices for Case A (independent input variables).

$\mathbf{X}_u$	Monte Carlo $N = 10^6$, $R = 10^2$		Quasi-Monte Carlo $N = 10^6$, $R = 10^2$		Sparse Grid $\ell = 4$, $N = 56785$	
	$10^2 \times S_{\mathbf{X}_u}$	$10^2 \times S^{\text{tot}}_{\mathbf{X}_u}$	$10^2 \times S_{\mathbf{X}_u}$	$10^2 \times S^{\text{tot}}_{\mathbf{X}_u}$	$10^2 \times S_{\mathbf{X}_u}$	$10^2 \times S^{\text{tot}}_{\mathbf{X}_u}$
Σ_c^1	17.66	17.66	17.66	17.66	17.66	17.66
Σ_c^2	16.24	16.26	16.26	16.26	16.26	16.26
Σ_f^1	0.71	0.72	0.72	0.72	0.72	0.72
Σ_f^2	6.40	6.41	6.41	6.41	6.41	6.41
$\nu\Sigma_f^1$	8.07	8.08	8.08	8.08	8.08	8.08
$\nu\Sigma_f^2$	46.76	46.78	46.77	46.77	46.77	46.77
$\Sigma_s^{1\to 2}$	4.09	4.10	4.10	4.10	4.10	4.10

Considering the results of Case A, reported on in Table 4.6, the input variable with the greatest influence on the infinite neutron multiplication factor is the thermal neutron production ($\nu\Sigma_f^2$), and the input variable with the least influence is the fast neutron fission (Σ_f^1). This is similar to what we anticipated, given the fact that the infinite neutron multiplication factor is highly dependent on the number of neutrons produced in the system. Since the system being considered is thermal, the thermal neutron production should account for most of the neutrons produced, and the effect of fast neutron fission was not expected to be significant.

Table 4.7: Sensitivity indices for Case B (block diagonal).

$\mathbf{X}_u$	Monte Carlo $N = 10^6,\ R = 10^2$		Quasi-Monte Carlo $N = 10^6,\ R = 10^2$		Sparse Grid $\ell = 4,\ N = 56785$	
	$10^2 \times S_{\mathbf{X}_u}$	$10^2 \times S^{\text{tot}}_{\mathbf{X}_u}$	$10^2 \times S_{\mathbf{X}_u}$	$10^2 \times S^{\text{tot}}_{\mathbf{X}_u}$	$10^2 \times S_{\mathbf{X}_u}$	$10^2 \times S^{\text{tot}}_{\mathbf{X}_u}$
$\left(\Sigma_c^1\ \Sigma_c^2\ \Sigma_f^1\ \Sigma_f^2\right)^T$	34.53	34.53	34.53	34.53	34.53	34.53
$\left(\nu\Sigma_f^1\ \nu\Sigma_f^2\right)^T$	61.24	61.26	61.25	61.25	61.25	61.25
$\left(\Sigma_s^{1\to 2}\right)$	4.20	4.22	4.22	4.22	4.21	4.21

The results for Case B are reported on in Table 4.7, and the subset $\{\nu\Sigma_f^1, \nu\Sigma_f^2\}$, which corresponds to the neutron production, had the greatest influence on the infinite neutron multiplication factor. The subset $\{\Sigma_s^{1\to 2}\}$, which corresponds to the fast neutron removal, was the least influential. It should be noted that the value of the sensitivity index for $\{\Sigma_s^{1\to 2}\}$ is different in Tables 4.6 and 4.7. This is because the off-diagonal terms of the covariance matrix influences the results for $\{\Sigma_s^{1\to 2}\}$ in Table 4.7. In other words, due to the off-diagonal terms in the correlation matrix, Cases A and B define different problems.

The results of the sensitivity indices for cases A and B, in Tables 4.6 and 4.7, were obtained by using a high number of samples with all three numerical quadratures, and these results are taken as the reference. There seems to be very good agreement of the computed sensitivity indices between all three quadratures. The accuracy obtained for the reference results is much better than the accuracy needed to draw practical conclusions concerning the contribution of different uncertainties. By this we mean, that the accuracy of the sensitivity index estimation has to be, at least, sufficient to discriminate between the contribution of different inputs, and should also be able to discriminate between $S^{\text{tot}}_{\mathbf{X}_u}$ and $S_{\mathbf{X}_u}$ for a given input $\mathbf{X}_u$. Therefore, an error estimation study was done, in order to determine the influence of the number of samples on the absolute and relative quadrature error of the computed sensitivity indices, where the relative quadrature error is given by

$$\hat{\delta} = \frac{\hat{\epsilon}_{(RN/\ell)}\left(S^{(\mathrm{tot})}_{\mathbf{X}_u}\right)}{S^{(\mathrm{tot})}_{\mathbf{X}_u}} \times 100 \ [\%]. \tag{4.10}$$

This study will help in approximating the number of samples that is needed to get a good estimation of the sensitivity indices with the different numerical methods. For Monte Carlo and quasi-Monte Carlo methods, three different sample sizes were considered, $N = 10^2$, $N = 10^4$ and $N = 10^6$. In all the cases the number of independent sequences R was taken as 10^2. For the sparse grid, levels $\ell = 1$ to $\ell = 4$ were considered.

It was observed in both cases that the results obtained for $S^{\mathrm{tot}}_{\mathbf{X}_u}$ and $S_{\mathbf{X}_u}$ are statistically similar for all the subsets of the input variables, for all three the numerical methods that were used. This implies that the interaction effects can be neglected. It was also observed that the integration error for $S^{\mathrm{tot}}_{\mathbf{X}_u}$ was smaller than for $S_{\mathbf{X}_u}$ in all the cases, hence from now on, we will only consider $S^{\mathrm{tot}}_{\mathbf{X}_u}$.

When considering Case A, it was observed that increasing N by a factor of 10^2, resulted in a reduction of the integration error by a factor of approximately 10 for all the computed total sensitivity indices when using Monte Carlo. The results for quasi-Monte Carlo showed that increasing N from 10^2 to 10^4, and subsequently from 10^4 to 10^6, resulted in a decrease of the integration error by a factor of about 30 and 40 respectively for all the computed total sensitivity indices. For the sparse grid, a level change from $\ell = 2$ to $\ell = 3$, and from $\ell = 3$ to $\ell = 4$ both resulted in a decrease of the integration error by a factor of about 3. The maximum absolute and relative errors for the total sensitivity indices computed with different quadratures are reported on in Tables 4.8 to 4.11. These maximum absolute errors are obtained by taking the maximal absolute error of all the sensitivity indices for a given case, a given number of samples and a given quadrature. The maximum relative error is obtained in the same way.

As one can see from Tables 4.8 and 4.10, a relatively small number of samples (100×100) in the case of Monte Carlo gave fairly good accuracy (about 2%) in the estimation of the total sensitivity indices. It should be noted that levels $\ell = 0$ and $\ell = 1$ for the sparse grid were not considered in the error estimation. This is because for level $\ell = 0$, the abscissa consists of only one point, and the variance is zero, hence the total sensitivity index will be undefined. For the same reason the application of Eq. (4.5) cannot give reasonable results for level $\ell = 1$. However, looking at

Tables 4.9 and 4.11, it can be seen that the maximal difference (i.e. before multiplication by a factor 100) between the results obtained for levels $\ell = 1$ and $\ell = 2$ is smaller than 2×10^{-5}, and the maximum relative quadrature error obtained when moving from level $\ell = 1$ to $\ell = 2$ is smaller than 3.8×10^{-2}%. Hence this shows that for both cases, level $\ell = 1$ which contains only 29 points, is sufficient to estimate the total sensitivity indices with a very good accuracy.

Table 4.8: Maximum error of Monte Carlo and quasi-Monte Carlo quadratures in Case A.

Number of Samples	Monte Carlo		Quasi-Monte Carlo	
	$10^2 \times \hat{\epsilon}_{RN}$	$\hat{\delta}$ (%)	$10^2 \times \hat{\epsilon}_{RN}$	$\hat{\delta}$ (%)
$N = 10^2$, $R = 10^2$	9.0×10^{-1}	2.2	7.4×10^{-1}	1.6
$N = 10^4$, $R = 10^2$	8.0×10^{-2}	1.9×10^{-1}	2.7×10^{-2}	5.8×10^{-2}
$N = 10^6$, $R = 10^2$	7.8×10^{-3}	2.0×10^{-2}	6.8×10^{-4}	1.8×10^{-3}

Table 4.9: Maximum error for the sparse grid quadrature in Case A.

ℓ	N	$10^2 \times \hat{\epsilon}_\ell$	$\hat{\delta}$ (%)
1	29	N/A	N/A
2	477	2.0×10^{-3}	3.8×10^{-2}
3	5769	6.4×10^{-4}	1.3×10^{-2}
4	56785	2.0×10^{-4}	4.1×10^{-3}

The relatively small number of sparse grid points needed for an accurate estimation of the sensitivity indices as well as the absence of interactions between input variables (as discussed above) was unexpected. This result can potentially be explained in the following way: the uncertainty in cross-sections is so small that only the vicinity of the cross-section mean values contribute to the integrals used in the estimation of sensitivity indices. In this vicinity the infinite neutron multiplication factor, which is used as the example, can be approximated with a fairy linear function.

Table 4.10: Maximum error of Monte Carlo and quasi-Monte Carlo quadratures in Case B.

Number	Monte Carlo		Quasi-Monte Carlo	
of Samples	$10^2 \times \hat{\epsilon}_{RN}$	$\hat{\delta}$ (%)	$10^2 \times \hat{\epsilon}_{RN}$	$\hat{\delta}$ (%)
$N = 10^2,\ R = 10^2$	1.2	2.1	9.8×10^{-1}	1.6
$N = 10^4,\ R = 10^2$	1.1×10^{-1}	1.9×10^{-1}	3.5×10^{-2}	5.8×10^{-2}
$N = 10^6,\ R = 10^2$	9.1×10^{-3}	2.0×10^{-2}	1.2×10^{-3}	1.9×10^{-3}

Table 4.11: Maximum error for the sparse grid quadrature in Case B.

ℓ	N	$10^2 \times \hat{\epsilon}_\ell$	$\hat{\delta}$ (%)
1	29	N/A	N/A
2	477	1.3×10^{-3}	3.0×10^{-2}
3	5769	4.3×10^{-4}	1.0×10^{-2}
4	56785	1.4×10^{-4}	3.6×10^{-3}

A small theoretical study was done to clarify this aspect. The standard deviations given in Table 4.4 were initially multiplied by arbitrary factors between 1 and 10 and, in the second phase, by arbitrary factors between 1 and 20, and the sensitivity indices were recalculated. These factors were chosen to make the effect of a wider distribution more prominent without introducing a significant non-physical effect due to negative cross-section values at the left tail of the distributions. It was observed that as the values of the standard deviations increase, interaction effects can be observed, i.e. $S^{\text{tot}}_{\mathbf{X}_u}$ becomes statistically different from $S_{\mathbf{X}_u}$. Furthermore, a larger number of points (higher levels) is needed to achieve the same accuracy as in the reference case. These results may be used to confirm our assumption on the nature of the good performance of the sparse grid quadrature. Nevertheless, a proper theoretical study is necessary to confirm our conclusion. The result of this theoretical study may have important practical implications in implementing the global sensitivity analysis in reactor calculations.

Chapter 5

Conclusion

A modified variance-based global sensitivity analysis technique that allows one to deal with input variables that are block-wise correlated and normally distributed, is presented. The focus of this study was the application of the modified technique to calculations of reactor parameters that are dependent on groupwise neutron cross-sections. It was assumed that the cross-sections are normally distributed random variables with known means and covariance matrices. The theoretical and mathematical aspects of the calculation of the global sensitivity indices under the above assumptions have been discussed. The problem of practical numerical calculations of the variance-based global sensitivity indices was addressed, namely different options for numerical integration were considered. A consistent overall path for the calculation of sensitivity indices was proposed and described.

A Fortran program was written to implement all the steps of the modified technique. The Fortran program has the capability to be coupled to any model code that a scientist/engineer is interested in, and can, in addition to performing sensitivity analysis, be used for model design optimization, uncertainty estimation in model parameters, as well as for the determination of target accuracy requirements. An example to demonstrate the accuracy of the sensitivity analysis results produced by the Fortran program was also presented. The modified technique was successfully implemented in practice and was tested on a problem that involved two-group assembly homogenised cross-sections as input variables. The performance of different numerical integration techniques was tested on a reactor problem with arbitrary, but realistic two-group cross-sections and covariance matrices. Different implementations gave consistent results for the test problem under consideration. The implementation based on sparse grid quadrature demonstrated the best accuracy with as low as a few dozen samples.

This good performance of sparse grid integration was not expected and a special mini-study was performed with the purpose of explaining its origin as well as the absence of interactions in the obtained sensitivity indices. The results of this study confirmed our hypothesis that the observed results can be explained by the very small cross-section uncertainty. Nevertheless, this conclusion still has to be supported by a theoretical explanation.

From a methodological point of view, the method presented in the paper is applicable to problems with an arbitrary number of input variables. Nevertheless, one has to be cautious when dealing with multivariate problems in order to escape the curse of dimensionality. In this work the applicability of our method to a few-group problem was demonstrated.

This is an ongoing research, and the next phase of this research will involve the application of the methodology to multigroup reactor problems by coupling the Fortran program to a general neutron transport solver such as SCALE. The coupling to an advanced program such as SCALE would require lots of testing, verification and validation, which would not be possible to complete within the time-frame required for a Master's mini-dissertation.

A specific potential beneficiary of this study will be the OSCAR code system, developed by the Radiation and Reactor Theory group of the South African Nuclear Energy Corporation (Necsa). Necsa is the operator of South African's research reactor SAFARI-1, and is presently the largest producer of medical isotopes. The OSCAR code system is a cutting edge reactor neutronic calculational system used for research reactor modelling, in particular material test reactors. The Fortran program has the potential of being incorporated as a sensitivity analysis module in the OSCAR code system.

The most important results relating to this mini-dissertation has been reported in:

1. P.M. Bokov and B.A. Adetula. Block-wise Global Sensitivity/Uncertainty Analysis Depending on Multi-Group Neutron Cross-Sections. Technical Report RRT-OSCAR-REP-10001, Necsa, South Africa, March 2010.

2. P.M. Bokov and B.A. Adetula. An Algorithm for Global Sensitivity Analysis Applicable to

Exercise I-1. In *Uncertainty Analysis and Modelling (UAM-4) Workshop*, Pisa, Italy, 14 – 16 April 2010.

3. B.A. Adetula and P.M. Bokov. Efficiency of Different Numerical Techniques for Evaluating Global Sensitivity Indices when Input Variables are Correlated and Normally Distributed. In *SAIP Annual Conference*, CSIR, Pretoria, South Africa, 27 September – 1 October 2010.

4. B.A. Adetula and P.M. Bokov. Method for Calculation of Global Sensitivity Indices for Few-Group Cross-Section Dependent Problems. In *International Conference on Mathematics and Computational Methods Applied to Nuclear Science and Engineering*, Rio de Janeiro, Brazil, 8 – 12 May 2011.

Bibliography

[1] A. Saltelli. Sensitivity Analysis for Importance Assessment. *Risk Analysis*, 22(3):579–590, 2002.

[2] A. Saltelli, et al. *Global Sensitivity Analysis. The Primer.* John Wiley & Sons, England, 2008.

[3] T. Takeda, K. Asano and T. Kitada. Sensitivity Analysis Based on Transport Theory. *Journal of Nuclear Science and Technology*, 43(7):743–749, 2006.

[4] G. Palmiotti, M. Salvatores and G. Alberti. Methods in Use for Sensitivity Analysis, Uncertainty Evaluation, and Target Accuracy Assessment. In *4th Workshop on Neutron Measurements, Evaluations and Applications*, Prague, Czech Republic, 16 - 18 October 2007.

[5] G. Aliberti, et al. Nuclear Data Sensitivity, Uncertainty and Target Accuracy Assessment for Future Nuclear Systems. *Annals of Nuclear Energy*, 33:700–733, 2006.

[6] J. Jacques, C. Lavergne and N. Devictor. Sensitivity Analysis in the Presence of Model Uncertainty and Correlated Inputs. *Reliability Engineering and System Safety*, 91(10-11):1126–1134, 2006.

[7] E. Volkova, B. Iooss and F. Van Dorpe. Global Sensitivity Analysis for a Numerical Model of Radionuclide Migration from the Kurchatov Institute Radwaste Disposal Site. *Stochastic Environmental Research and Risk Assessment*, 22(1):17–31, 2008.

[8] B. Iooss and M. Ribatet. Global Sensitivity Analysis of Computer Models with Functional Inputs. *Reliability Engineering and System Safety*, 94(7):1194–1204, 2009.

[9] I.M. Sobol'. Global Sensitivity Indices for Nonlinear Mathematical Models and their Monte Carlo Estimates. *Mathematics and Computers in Simulation*, 55:271–280, 2001.

[10] U. Reuter and M. Liebscher. Global Sensitivity Analysis in View of Nonlinear Structural Behavior. In *2008 German Conference organized by DYNAmore GmbH, LS-DYNA Anwenderforum*, Bamberg, Germany, October 2008.

[11] B. Sudret. Global Sensitivity Analysis using Polynomial Chaos Expansions. *Reliability Engineering and System Safety*, 93(7):964–979, 2008.

[12] M. Herman and A. Trkov. *ENDF-6 Formats Manual; CSEWG Document ENDF-102, Report BNL-90365-2009 Rev.1.* National Nuclear Data Center, Brookhaven National Laboratory, Upton, USA, July 2010.

[13] K. Ivanov, et al. Benchmark for Uncertainty Analysis in Modeling (UAM) for Design, Operation and Safety Analysis of LWRs. Technical Report NEA/NSC/DOC(2007)23, OECD Nuclear Energy Agency, France, December 2007.

[14] H.W. Bode. *Network Analysis and Feedback Amplifier Design.* Van Nostrand-Reinhold, Princeton, New Jersey, 1945.

[15] G.B. Dantzig. *Linear Programming and Extensions.* Princeton University Press, Princeton, New Jersey, 1963.

[16] T. Gal. *Postoptimality Analyses, Parametric Programming and Related Topics.* McGraw-Hill, Great Britain, 1979.

[17] J.E. Ward and R.E. Wendell. Approaches to Sensitivity Analysis in Linear Programming. *Annals Operational Research*, (27):3–38, 1990.

[18] N. Ludtke, et al. Information-Theoretic Sensitivity Analysis: A General Method For Credit Assignment in Complex Network. *Journal of The Royal Society Interface*, 5:223–225, 2008.

[19] R. Tomovic and M. Vucobratovic. *General Sensitivity Theory.* Elsevier, New York, 1972.

[20] P.M. Frank. *Introduction to System Sensitivity Theory.* Academic, New York, 1978.

[21] A. Saltelli, et al. *Sensitivity Analysis in Practice: A Guide to Assessing Scientific Models.* John Wiley & Sons, England, 2004.

[22] D.G. Cacuci. *Sensitivity and Uncertainty Analysis: Vol I, Theory.* Chapman and Hall/CRC Press, Boca Raton, Florida, 2003.

[23] D.G. Cacuci. Sensitivity and Uncertainty Analysis of Models and Data. In Y. Azmy and E. Sartori, editors, *Nuclear Computational Science: A Century in Review*, pages 291–353. Springer, London, 2010.

[24] D. Shirley and W. Stanley. *Statistics for Research*. John Wiley & Sons, New York, 1983.

[25] B.A. Berg. *Markov Chain Monte Carlo Simulations and Their Statistical Analysis: With Web-based Fortran Code*. World Scientific Publishing Co. Pte. Ltd, Singapore, 2004.

[26] R.A. Johnson and D.W. Wichern. *Applied Multivariate Statistical Analysis*. Pearson Prentice Hall, Upper Saddle River, New Jersey, 6th edition, 2007.

[27] P. Newbold. *Statistics for Business and Economics*. Prentice Hall, Englewood Cliffs, New Jersey, 2nd edition, 1988.

[28] K.O. Arras. An Introduction to Error Propagation: Derivation, Meaning and Examples. Technical Report EPFL-ASL-TR-98-01 R3, Autonomous Systems Lab, Institute of Robotic Systems, Swiss Federal Institute of Technology, Lausanne, Switzerland, September 1998.

[29] N.R. Draper and H. Smith. *Applied Regression Analysis*. John Wiley & Sons, New York, 1981.

[30] R.L. Iman and J.C. Helton. An Investigation of Uncertainty and Sensitivity Analysis Techniques for Computer Models. *Risk Analysis*, 8:71–90, 1988.

[31] J.C. Helton. Uncertainty and Sensitivity Analysis Techniques for Use in Performance Assessment for Radioactive Waste Disposal. *Reliability Engineering System Safety*, 42:327–367, 1993.

[32] C. Daniel. One-at-a-Time-Plans. *Journal of American Statistical Association*, 68:353–360, 1973.

[33] R.A. Fischer. *The Design of Experiments*. Oliver and Boyd, Edinburgh, 1935.

[34] G.E.P. Box, W.G. Hunter and J.S. Hunter. *Statistics for Experimenters*. John Wiley & Sons, New York, 1978.

[35] A.H. Ang and W.H Tang. *Probability Concepts in Engineering Planning and Design, Vol II*. John Wiley & Sons, New York, 1984.

[36] K. Breitung. Asymptotic Approximation for Multi Normal Integrals. *Journal of Engineering Mechanics*, 110(3):357–366, 1984.

[37] Y.G. Zhao and T. Ono. A General Procedure for FORM/SORM. *Structural Safety*, 21(2):95–112, 1999.

[38] Y.T. Wu, H.R. Millwater and T.A. Cruse. Advanced Probabilistic Structural Analysis Method for Implicit Performance Functions. *Journal of American Institute of Aeronautics and Astronautics*, 28(9):1663–1669, 1990.

[39] S. Xu and R.V. Grandhi. Effective Two-Point Function Approximation for Design Optimization. *Journal of American Institute of Aeronautics and Astronautics*, 36(12):2269–2275, 1998.

[40] L. Cizelj, B. Mavko and H. Riesch-Oppermann. Application of First and Second Order Reliability Methods in Safety Assessment of Cracked Steam Generators Tubing. *Nuclear Engineering and Design*, 147:1–9, 1994.

[41] Y.G. Zhao, T. Ono and M. Kato. Second Order Third Moment Reliability Method. *Journal of Structural Engineering*, 128(8):1087–1090, 2002.

[42] H.O. Madsen, S. Krenk and N.C. Lind. *Methods of Structural Safety.* Prentice Hall, Englewood Cliffs, New Jersey, 1986.

[43] M.H. Holmes. *Introduction to Perturbation Methods.* Springer, New York, 1995.

[44] L. Vuilleumier, R.A. Harvey and N.J. Brown. First and Second Order Sensitivity Analysis of a Photochemically Reactive System: A Green's Function Approach. *Environmental Science and Technology*, 31(4):1206–1217, 1997.

[45] K. Chan, A. Saltelli and S. Tarantola. Sensitivity Analysis of Model Output: Variance Based Methods Make the Difference. In *Proceeding of the 1997 Winter Simulation Conference*, pages 261–268, Atlanta, Georgia, 7 - 10 December 1997.

[46] M.D. McKay. Non-Parametric Variance Based Methods of Assessing Uncertainty Importance. *Reliability Engineering and Safety System*, 57:267–269, 1997.

[47] S.C. Hora and R.L. Iman. A Comparison of Maximum/Bounding and Bayesian/Monte Carlo for Fault Tree Uncertainty Analysis. Technical Report SAND85-2839, Sandia National Laboratories, USA, 1989.

[48] R.L. Iman and S.C. Homma. A Robust Measure of Uncertainty Importance for Use in Fault Tree System Analysis. *Risk Analysis*, 10:410–406, 1990.

[49] B. Krzykacz-Hausmann. The Principal Variance-Based Sensitivity Indices can be Estimated by The"Ishigami-Homma-Saltelli" Method without Assuming Independence between the Input Variables. In *Fifth International Conference on Sensitivity Analysis on Model Output*, Budapest, Hungary, 18 - 22 June 2007.

[50] R.I. Cukier, et al. Study of the Sensitivity of Coupled Reactions Systems to Uncertainties in Rate Coefficients: I Theory. *Journal of Chemical Physics*, 59(8):3873–3878, 1973.

[51] R.I. Cukier, H.B. Levine and K.E. Shuler. Nonlinear Sensitivity Analysis of Multi Parameter Model Systems. *Journal of Computational Physics*, 26:1–42, 1978.

[52] A. Saltelli, S. Tarantola and K.P. Chan. A Quantitative Model Independent Method for Global Sensitivity Analysis of Model Output. *Technometrics*, 41(1):39–56, 1999.

[53] H. Weyl. Mean Motion. *American Journal of Mathematics*, 60(4):889–896, 1938.

[54] D.J.C. MacKay. *Information Theory, Inference and Learning Algorithms.* Cambridge University Press, Cambridge, United Kingdom, 2005.

[55] C.E. Shannon and W. Weaver. *The Mathematical Theory of Communication.* University of Illinois Press, Urbana, Illinois, 1949.

[56] B. Auder and B. Iooss. Global Sensitivity Analysis Based on Entropy. In S. Martorell, C.G. Soares and J. Barnett, editors, *Safety, Reliability and Risk Analysis: Theory Methods and Applications*, pages 2107–2115. Taylor and Francis Group, London, 2009.

[57] H. Liu, W. Chen and A. Sudjianto. Relative Entropy Based Method for Probabilistic Sensitivity Analysis in Engineering Design. *ASME Journal of Mechanical Design*, 128:326–336, 2006.

[58] M. Lejeune. *La Theorie et Ses Applications.* Springer Verlag, Paris, 2004.

[59] L. Leal, et al. Impact of the U-235 Covariance Data in Benchmark Calculations. In *International Conference on the Physics of Reactors "Nuclear Power: A Sustainable Resource"*, Interlaken, Switzerland, 14 - 19 September 2008.

[60] W. Zwermann, et al. Influence of Nuclear Covariance Data on Reactor Core Calculations. In *WONDER Conference*, Cadarache, France, 29 September - 2 October 2009.

[61] R.W. Peelle and T.W. Burrows. An Annotated Bibliography Covering Generation and Use of Evaluated Cross Section Uncertainty Files. Technical Report BNL-NCS-51684, Brookhaven National Laboratory, USA, March 1983.

[62] M. Salvatores and R. Jacqmin. Uncertainty and Target Accuracy Assessment for Innovative Systems using Recent Covariance Data Evaluations, Vol 26. Technical Report NEA/WPEC-26, OECD Nuclear Energy Agency, France, 2008.

[63] M.L. Williams, et al. *SCALE Nuclear Data Covariance Library; ORNL/TM-2005/39, Version 6, Vol III, Sect. M19.* Oak Ridge National Laboratory, Tennessee, USA, January 2009.

[64] A. Weinberg and E. Wigner. *The Physical Theory of Neutron Chain Reactors.* University of Chicago Press, Chicago, 1958.

[65] B.T. Rearden, et al. *TSUNAMI Primer: A Primer for Sensitivity/Uncertainty Calculations with SCALE; ORNL/TM-2009/027.* Oak Ridge National Laboratory, Tennessee, USA, January 2009.

[66] M.L. William, B.L. Broadhead and C.V. Parks. Eigenvalue Sensitivity Theory for Resonance Shielded Cross Sections. *Nuclear Science and Engineering*, 138:177–191, 2001.

[67] G. Rimpault, et al. The ERANOS Code and Data System for Fast Reactor Neutronic Analyses. In *International Conference on the New Frontiers of Nuclear Technology: Reactor Physics, Safety and High-Performance Computing*, Seoul, Korea, 7 - 10 October 2002.

[68] M. Eaton and M.M.R. Williams. A Probabilistic Study of the Influence of Parameter Uncertainty on Solutions of the Neutron Transport Equation. *Progress in Nuclear Energy*, 52:580–588, 2010.

[69] T.E. Booth, et al. *MCNP - A General Monte Carlo N-Particle Transport Code, Version 5, Volume II: User Guide; LA-CP-03-0245.* Los Alamos National Laboratory, New Mexico, USA, April 2003.

[70] F. Puente-Espel, et al. Application of Global Sensitivity Analysis Approach to Exercise I-1 of the OECD LWR UAM Benchmark. In *Computational Methods and Reactor Physics*, Saratoga Springs, New York, USA, 3 - 7 May 2009.

[71] G. Marsaglia, Z. Wai and W. Tsang. Toward a Universal Random Number Generator. *Statistics & Probability Letters*, 9(1):35–39, 1990.

[72] Y.A. Shreider, et al. *Monte Carlo Method.* Pergamon Press, Oxford, 1966.

[73] M.H. Kalos and P.A. Whitlock. *Monte Carlo Methods.* Wiley-VCH, Germany, 2nd edition, 2008.

[74] W.H. Press, et al. *Numerical Recipes in Fortran 77. The Art of Scientific Computing.* Cambridge University Press, Cambridge, United Kingdom, 1999.

[75] I. Krykova. Evaluating of Path-Dependent Securities With Low Discrepancy Methods. Master's thesis, Worcester Polytechnic Institute, Massachusetts, USA, 2003.

[76] J.E. Gentle. *Random Number Generation and Monte Carlo Methods.* Springer, New York, 2nd edition, 2003.

[77] A.B. Owen. Monte Carlo Extension of Quasi-Monte Carlo. In *Proceedings of the 30th Conference on Winter Simulation*, pages 571–577, Washington DC, USA, 13 - 16 December 1998.

[78] J. Burkardt. An Introduction to High Dimensional Sparse Grids. A Talk given at the Mathematics Department of Ajou University, Suwon, Korea. 11 May 2009.

[79] S.A. Smolyak. Quadrature and Interpolation Formulas for Tensor Products of Certain Classes of Functions. *Dokl. Akad. Nauk SSSR*, 4:240–243, 1963.

[80] R. Zivanovic. Cross-Section Parameterization via Sparse Grids; Feasibility Study Report. Technical Report RRT-FMR-06-04, Necsa, South Africa, November 2006.

[81] V. Barthelmann, E. Novak and K. Ritter. High Dimensional Polynomial Interpolation on Sparse Grids. *Advances in Computational Mathematics*, 12:273–288, 2000.

[82] A. Klimke and B. Wohlmuth. Algorithm 847: Spinterp: Piecewise Multilinear Hierarchical Sparse Grid Interpolation in Mathlab. *ACM Transactions on Mathematical Software*, 4(4):561–579, 2005.

[83] I.M. Sobol'. Sensitivity Estimates for Nonlinear Mathematical Models. *Mathematical Modelling and Computational Experiment*, 1:407–414, 1993.

[84] A. Saltelli and I.M. Sobol'. Sensitivity Analysis for Nonlinear Mathematical Models: Numerical Experience. *Matematicheskoe Modelirovanie*, 7(11):16–28, 1995.

[85] W. Mauntz and S. Kucherenko. Application of Global Sensitivity Indices for Measuring the Effectiveness of Quasi-Monte Carlo Method. *In Press*, 2007.

[86] E. Novak and K. Ritter. High Dimensional Integration of Smooth Functions over Cubes. *Numerische Mathematik*, 75(1):240–243, 1996.

[87] E. Novak. Simple Cubature Formulas with High Polynomial Exactness. *Constructive Approximation*, 15(4):499–522, 1999.

[88] G.E.P. Box and M.E. Muller. A Note on the Generation of Random Normal Deviates. *The Annals of Mathematical Statistics*, 29(2):610–611, 1958.

[89] B. Moro. The Full Monte. *Risk*, 8(2):57–58, 1995.

[90] J. Burkardt. Source Codes in Fortran90 [Online]. Avaliable from: <http://people.sc.fsu.edu/~jburkardt/f_src/f_src.html>, [Accessed February 2011].

[91] S. Kucherenko and N. Shah. The Importance of being Global. Application of Global Sensitivity Analysis in Monte Carlo Option Pricing. *Wilmott Magazine*, 4:2–10, 2007.

[92] J. Waldvogel. Fast Construction of Fejer and Clenshaw-Curtis Quadrature Rules. *BIT Numerical Mathematics*, 43(1):1–18, 2003.

[93] T. Gerstner and M. Griebel. Numerical Integration Using Sparse Grids. *Numerical Algorithms*, 18(3-4):208–232, 1998.

[94] M. Williams, et al. Sensitivity/Uncertainty Analysis for OECD UAM Benchmark of Peach Bottom BWR. In *Uncertainty Analysis and Modelling (UAM-4) Workshop*, Pisa, Italy, 14 -16 April 2010.

[95] W. M. Stacey. *Nuclear Reactor Physics.* John Wiley & Sons, New York, USA, 2001.

Appendix A

Approximation of Multidimensional Integrals with Sparse Grid Quadratures

Let $\varphi : \Omega \to \mathbb{R}$ be a continuous function of its arguments $(x_1, \ldots, x_d)$, with bounded mixed derivatives of order r:

$$\left\| \frac{\partial^{\|k\|_1} \varphi\left(x_1, \ldots, x_d\right)}{\partial x_1^{k_1} \cdots \partial x_d^{k_d}} \right\|_\infty < \infty, \quad k_i \leq r, \tag{A.1}$$

where d is the dimensionality of the problem, $\|k\|_1 = k_1 + \cdots + k_d$, $\Omega = \Omega_1 \times \cdots \times \Omega_d$, and $\Omega_i \subset \mathbb{R}$ $(i = 1, 2, \ldots, d)$ are bounded or unbounded intervals. We consider an approximation to the integral

$$I\left[\varphi\left(\mathbf{x}\right)\right] = \int_\Omega \varphi\left(\mathbf{x}\right) \varrho\left(\mathbf{x}\right) \mathrm{d}\mathbf{x}, \tag{A.2}$$

where $\mathbf{x} = (x_1, \ldots, x_d)$, and the weight function is expressed in tensor product form $\varrho\left(\mathbf{x}\right) = \varrho_1\left(x_1\right) \cdots \varrho_d\left(x_d\right)$.

In order to construct a multidimensional sparse grid quadrature, let us first consider a sequence of univariate quadrature formulas

$$Q_{l_i}\left[\psi\left(x_i\right)\right] = \sum_{j=1}^{m_{l_i}} w_{j_i}^{l_i} \psi\left(x_{j_i}^{l_i}\right), \tag{A.3}$$

which approximate one-dimensional integrals

$$\int_{\Omega_i} \psi\left(x_i\right) \varrho_i\left(x_i\right) \mathrm{d}x_i, \quad i = 1, 2, \ldots, d. \tag{A.4}$$

Here $\psi : \Omega_i \to \mathbb{R}$ is a continuous function of its argument, x_i, $l_i \in \mathbb{Z}$ is the accuracy level of the quadrature formula where $l_i \geq 0$, m_{l_i} is the number of abscissas (knots) $x_{j_i}^{l_i}$ of the quadrature and $w_{j_i}^{l_i}$ is the corresponding weight. The index l_i is written explicitly over abscissas and weights, in order to remind one that they may change for different levels. $\mathcal{H}_{l_i} = \left\{x_{j_i}^{l_i} : 1 \leq j_i \leq m_{l_i}\right\}$ will be used to denote the set of knots of the one-dimensional quadrature formula.

In the sparse grid method the integral Eq. (A.2) is approximated via the Smolyak formula [79, 86], defined for an accuracy level $\ell \in \mathbb{Z}$ ($\ell \geq 0$) of the sparse grid as follows:

$$Q_{\ell,d}\left[\varphi\left(\mathbf{x}\right)\right] = \sum_{\ell-d+1 \leq \|\mathbf{l}\|_1 \leq \ell} \left(-1\right)^{\ell-\|\mathbf{l}\|_1} \binom{d-1}{\ell - \|\mathbf{l}\|_1} \bigotimes_{i=1}^{d} Q_{l_i}\left[\varphi\left(\mathbf{x}\right)\right], \tag{A.5}$$

where $\|\mathbf{l}\|_1 = \sum_{i=1}^{d} l_i$ and the multi-index $\mathbf{l} = (l_1, l_2, \ldots, l_d) \in \mathbb{Z}^d$ contains the accuracy level of the one-dimensional quadrature Eq. (A.3) for each dimension. The tensor product $\bigotimes$ in Eq. (A.5) can be calculated as

$$\bigotimes_{i=1}^{d} Q_{l_i}\left[\varphi\left(\mathbf{x}\right)\right] = \sum_{j_1=1}^{m_{l_1}} \cdots \sum_{j_d=1}^{m_{l_d}} \varphi\left(x_{j_1}^{l_1}, \ldots, x_{j_d}^{l_d}\right) \prod_{i=1}^{d} w_{j_i}^{l_i}, \tag{A.6}$$

where the tensor product of quadrature weights $w_{j_i}^{l_i}$ is replaced with the ordinary product, since they are real numbers. As one can see from the structure of Eqs. (A.5) and (A.6), quadrature $Q_{\ell,d}\left[\varphi\left(\mathbf{x}\right)\right]$ is a linear functional that depends on φ through function values at a finite set of points. This set of point is called a “sparse grid” and is denoted by $\mathcal{H}_{\ell,d}$. A sparse grid is defined as the union

$$\mathcal{H}_{\ell,d} = \bigcup_{\ell-d+1 \leq \|\mathbf{l}\|_1 \leq \ell} \left(\mathcal{H}_{l_1} \times \cdots \times \mathcal{H}_{l_d}\right). \tag{A.7}$$

For nested one-dimensional sets ($\mathcal{H}_{l_i} \subset \mathcal{H}_{l_i+1}$) the corresponding sparse grids are also nested $\mathcal{H}_{\ell,d} \subset \mathcal{H}_{\ell+1,d}$ and can be simplified, yielding

$$\mathcal{H}_{\ell,d} = \bigcup_{\|\mathbf{l}\|_1 = \ell} \left(\mathcal{H}_{l_1} \times \cdots \times \mathcal{H}_{l_d}\right). \tag{A.8}$$

The integral Eq. (A.2) can now be approximated by the sum:

$$Q_{\ell,d}\left[\varphi\left(\mathbf{x}\right)\right] = \sum_{\mathbf{x}_{\mathbf{j}}^{\mathbf{l}} \in \mathcal{H}_{\ell,d}} w_{\mathbf{j}}^{\mathbf{l}} \varphi\left(\mathbf{x}_{\mathbf{j}}^{\mathbf{l}}\right), \tag{A.9}$$

where multidimensional knots $\mathbf{x}_{\mathbf{j}}^{\mathbf{l}} = \left(x_{j_1}^{l_1}, x_{j_2}^{l_2}, \ldots, x_{j_d}^{l_d}\right)$ can be constructed based on Eqs. (A.7) and (A.8). The formulae for the quadrature weights $w_{\mathbf{j}}^{\mathbf{l}}$ in Eq. (A.9) can be obtained in an analytical form only in a few particular cases; in all the other cases, weights can be either precalculated or calculated online using Eqs. (A.5) and (A.6).